ORIGINAL RESEARCH

Modeling Treatment Response for Lamin A/C Related Dilated Cardiomyopathy in Human Induced Pluripotent Stem Cells

Yee-Ki Lee, PhD;* Yee-Man Lau, PhD;* Zhu-Jun Cai, MSc; Wing-Hon Lai, PhD; Lai-Yung Wong, BSc; Hung-Fat Tse, MD, PhD; Kwong-Man Ng, PhD; Chung-Wah Siu, MD

***Background*—**Precision medicine is an emerging approach to disease treatment and prevention that takes into account individual variability in the environment, lifestyle, and genetic makeup of patients. Patient-specific human induced pluripotent stem cells hold promise to transform precision medicine into real-life clinical practice. Lamin A/C (LMNA)-related cardiomyopathy is the most common inherited cardiomyopathy in which a substantial proportion of mutations in the *LMNA* gene are of nonsense mutation. PTC124 induces translational read-through over the premature stop codon and restores production of the full-length proteins from the affected genes. In this study we generated human induced pluripotent stem cells-derived cardiomyocytes from patients who harbored different *LMNA* mutations (nonsense and frameshift) to evaluate the potential therapeutic effects of PTC124 in *LMNA*-related cardiomyopathy.

***Methods and Results*—**We generated human induced pluripotent stem cells lines from 3 patients who carried distinctive mutations (R225X, Q354X, and T518fs) in the *LMNA* gene. The cardiomyocytes derived from these human induced pluripotent stem cells lines reproduced the pathophysiological hallmarks of *LMNA*-related cardiomyopathy. Interestingly, PTC124 treatment increased the production of full-length LMNA proteins in only the R225X mutant, not in other mutations. Functional evaluation experiments on the R225X mutant further demonstrated that PTC124 treatment not only reduced nuclear blebbing and electrical stress-induced apoptosis but also improved the excitation-contraction coupling of the affected cardiomyocytes.

***Conclusions*—**Using cardiomyocytes derived from human induced pluripotent stem cells carrying different *LMNA* mutations, we demonstrated that the effect of PTC124 is codon selective. A premature stop codon UGA appeared to be most responsive to PTC124 treatment. **(*J Am Heart Assoc*. 2017;6:e005677. DOI: 10.1161/JAHA.117.005677.)**

Key Words: dilated cardiomyopathy • lamin A/C cardiomyopathy • nonsense mutation • PTC124 • translational read through

Lamins A and C (Lamin A/C) are intermediate filament proteins encoded by the autosomal *LMNA* gene and constitute major components of the nuclear lamina.[1] Mutations in *LMNA* cause a wide spectrum of human diseases collectively referred to as "laminopathies,"[2-6] from multisystem involvement conditions such as Hutchinson Gilford progeria and muscular dystrophy to isolated dilated cardiomyopathy. *LMNA*-related cardiomyopathy is characterized by early-onset atrioventricular block and atrial fibrillation and subsequently progresses to ventricular tachyarrhythmia with consequent sudden cardiac death, left ventricular dysfunction, and heart failure. *LMNA* mutations are the most common cause of familial dilated cardiomyopathy, accounting for 5% to 10% of all cases and up to 30% to 45% of families with dilated cardiomyopathy and conduction system disease.[7,8] Despite a clear genetic basis, to date, no specific therapeutic strategies are available to modify the disease progression. In fact, the clinical management of *LMNA*-related dilated cardiomyopathy is no different from that for other forms of dilated cardiomyopathy. Genetically, LMNA-related cardiomyopathy is a dominant trait, and based on the results of mouse model, haploinsufficiency is likely the pathogenic mechanism.[9] One important implication of nonsense mutations is a therapeutic possibility of alleviating or even reversing the disease process by translational read-through of premature stop codons and production of full-length proteins by interfering with ribosomal proofreading. For instance, PTC124, also known as ataluren, discovered through

From the Cardiology Division, Department of Medicine, Li Ka Shing Faculty of Medicine, The University of Hong Kong, Hong Kong SAR, China.

Accompanying Table S1 and Figures S1 and S2 are available at http://jaha.ahajournals.org/content/6/8/e005677/DC1/embed/inline-supplementary-material-1.pdf

*Dr Lee and Dr Lau contributed equally to this work.

Correspondence to: Chung-Wah Siu, MD, or Kwong-Man Ng, PhD, Cardiology Division, Department of Medicine, The University of Hong Kong, Queen Mary Hospital, Hong Kong, China. E-mails: cwdsiu@hku.hk; skykmng@hku.hk

Received January 23, 2017; accepted May 2, 2017.

Clinical Perspective

What Is New?

- This is the first study of the read-through drug PTC124 in patient human induced pluripotent stem cells-derived cardiomyocytes for treatment of nonsense (UGA stop codon–specific) related cardiac laminopathy by recovery of expression of full-length Lamin A/C.

What Are the Clinical Implications?

- This study demonstrates the potential feasibility of human induced pluripotent stem cells-based precision medicine approaches to predict clinical responses of dilated cardiomyopathy patients and to study disease mechanisms.
- Drug testing in patient human induced pluripotent stem cells-derived cardiomyocytes may be a possible approach to select PTC124 responders for entry into clinical trials.

high-throughput screening utilizing premature UGA luciferase reporters to promote read-through of the premature stop codon,[10-12] has been granted orphan drug designation by the Food and Drug Administration in the United States for the treatment of nonsense mutation-related genetic disease. A phase 3 clinical trial is ongoing to evaluate the clinical efficacy of PTC124 in patients with nonsense mutation cystic fibrosis, which accounts for around 10% of cystic fibrosis cases.[13]

Notwithstanding the cost, standard randomized, double-blind, placebo-controlled studies might not always be possible because the number of patients with the same condition harboring the same or similar mutation is usually small. Human induced pluripotent stem cells (hiPSC) generated from individual patients who harbor a specific mutation have been exploited to elucidate the pathogenic mechanisms of various cardiovascular diseases.[14-19] The hiPSC technology is expected to revolutionize the concept of precision medicine by providing a steady supply of patient-specific functional cells for preclinical testing in order to identify the most effective and safest personalized strategies for a particular individual.[20] In fact, the US Food and Drug Administration has recently examined ways in which hiPSC-derived cardiomyocytes can be used in preclinical investigation of the potential risks in metabolic pathways or proarrhythmia events. Using hiPSC-derived cardiomyocytes generated from patients with *LMNA*-related cardiomyopathy, we have previously demonstrated that nuclear senescence and cell apoptosis are the key pathophysiological factors in *LMNA*-related cardiomyopathy.[18] In the present study we generated iPSCs from 3 patients with documented *LMNA*-related cardiomyopathy arising from 2 different nonsense mutations (UGA and UAG) and a frame-shift mutation in the *LMNA* gene. We differentiated them into cardiomyocytes to evaluate the effects of PTC124 on lamin A/C protein production, nuclear senescence, and cell apoptosis. Not only will our results allow us to differentiate a PTC124 responder from nonresponder to enter the clinical trials, but, more importantly, they demonstrate the feasibility of this iPSC-based precision medicine approach in studying genetic diseases.

Methods

Generation of hiPSC From Patients Carrying Cardiomyopathy-Associated *LMNA* Mutations

The study protocol for procurement of human tissue for the generation of hiPSCs was approved by the local Institutional Review Board and was registered at the Clinical Trial Center, the University of Hong Kong (IRB-UW08-258). After obtaining written informed consent from all participants, we collected skin biopsies. Skin biopsy samples were mechanically dissociated and plated onto 6-well culture dishes with the culture medium supplemented with 10% fetal bovine serum, as previously described.[21] Dermal fibroblasts growing out from the skin tissue were expanded and transduced with lentiviruses encoding human OCT4, SOX2, KLF4, and c-MYC. Putative hiPSC clusters were typically observed at 14 to 21 days after lentiviral transduction and were manually dissected and expanded onto new matrigel-coated 6-well plates. The authenticity of the hiPSCs was confirmed with the expression of a panel of pluripotent markers, transgene silencing, OCT4 promoter demethylation, and teratoma formation after inoculation into severe combined immunodeficiency mice (data not shown). All stem cell characterization works have been reported previously.[21]

Cardiac Differentiation

Cardiac differentiation of hiPSCs was induced using a previously reported protocol.[22] In brief, undifferentiated hiPSCs were maintained in mTeSRTM1 medium (STEMCELL Technologies Inc, Vancouver, BC, Canada). Four days before induction, hiPSCs were dissociated into single cells with accutase (Invitrogen, Carlsbad, CA) and then seeded onto a 12-well matrigel-coated plate (Thermo Scientific Inc, Waltham, MA) supplemented with Y27632 (5 μmol/L) (Stemgent, Cambridge, MA). On the first induction day the culture medium was switched to RPMI medium (Life Technologies, Carlsbad, CA) without insulin and supplemented with B27 (Life Technologies) and a GSK-β inhibitor, CHIR99021 (12 μmol/L) (Selleckchem, Houston, TX), and refreshed 24 hours later. On day 4, a Wnt signaling inhibitor, IWP2 (5 μmol/L) (Selleckchem, Houston, TX), was added to the culture medium. Typically, spontaneously beating cardiomyocytes were

observed around 9 days after induction. The cells were maintained in the cardiomyocyte maintenance medium (RPMI medium with B27 supplement) and used in subsequent analyses.

LMNA-Related Cardiomyopathy Model

The hiPSC-based model of *LMNA*-related cardiomyopathy was induced using electrical stimulation according to our previously published protocol.[18] Specifically, hiPSC-derived cardiomyocytes were seeded on 13-mm glass coverslips (Nunc A/S, Rockilde, Denmark) and mounted on a 6-well plate filled with corresponding medium. Electrical stimulation was then delivered to the cultured cells for 4 hours with carbon electrodes using an 8-channel C-Pace cell culture stimulator (IonOptix Co, Milton, MA) at 6.6 V/cm, 1 Hz, 2 milliseconds with alternating polarity. The total number of cells was counted before and after electrical stimulation.[23-25]

PTC124 Treatment

A stock solution of PTC124 was prepared by dissolving the lyophilized PTC124 (Selleckchem, Houston, TX) in DMSO to a concentration of 10 mmol/L. The stock solution was diluted in cell culture medium and preheated to 37°C to ensure complete dissolution before being applied to the cells. To test the potential therapeutic effects of PTC124, hiPSC-derived cardiomyocytes were pretreated with PTC124 (50 μmol/L) for 7 days before electrical stressing.

Western Blot Analysis

Western blot analysis was performed following the protocol described previously.[26] In brief, cells of interest were washed with Dulbecco phosphate-buffered saline and lysed in RIPA buffer (Cell Signaling Technology, Danvers, MA) containing 0.2% Triton X-100, 5 mmol/L EDTA, 1 mmol/L PMSF, 10 μg/mL leupeptin, 10 μg/mL aprotinin with additional 100 mmol/L NaF and 2 mmol/L Na_3VO_4. The supernatant was collected after spinning for 20 minutes at 12 000*g*. The amount of protein was quantified using a Bio-Rad protein assay kit (Hercules, CA). For each sample, 50 μg of total protein was resolved on a 4% to 12% Bis-Tris plus gel (Gibco, Gaithersburg, MD) and transferred onto nitrocellulose membranes. After blocking with 5% nonfat dry milk in TBS (pH 7.4) with 0.5% Tween-20 at 4°C, the transferred protein was probed by primary mouse monoclonal antibodies specific to lamin A/C (clone 4C-11; 1:2000; Cell Signaling Technologies, Danvers, MA). As an endogenous control, the levels of β-actin were evaluated using a monoclonal antibody specific to β-actin. The location of the immunoreactive protein complex was detected with HRP-conjugated secondary antibodies (Cell Signaling Technology, Danvers, MA; 1:2000) and visualized with standardized enhanced chemiluminescence systems.

Assessment of Nuclear Blebbing Events

At 30 to 40 days after induction of differentiation, hiPSC-derived cardiomyocytes were dissociated by collagenase treatment and subsequently seeded on gelatin-coated coverslips for immunostaining analysis and functional evaluation. For immunostaining, cells were fixed and permeabilized in 2% paraformaldehyde for 20 minutes at 4°C and then washed with wash buffer (Dulbecco phosphate-buffered saline with 0.1% Triton X-100; Sigma-Aldrich, St. Louis, MO). The nuclear lamina of hiPSC-derived cardiomyocytes was visualized by staining with antibodies specific to lamin A/C (clone 4C-11; 1:200; Cell Signaling Technologies, Danvers, MA) and cardiac-specific markers such as goat anti-tropoinin-T (1:400; Abcam, Cambridge, UK). Positively probed cells were visualized by addition of rabbit anti–goat IgG H+L Alexa 594 and rabbit anti–mouse IgG H+L Alexa 488 (Molecular Probes, Eugene, OR) for 30 minutes. Images were acquired using a fluorescence confocal Carl Zeiss LSM 700 microscope (Zeiss GmbH, Gottingen, Germany).

Terminal Deoxynucleotidyl Transferase dUTP Nick End Labeling Assay for Apoptosis

A terminal deoxynucleotidyl transferase dUTP nick end labeling (TUNEL) assay was performed using an in situ Cell Death Detection Kit, Fluorescein (Roche Applied Sciences, Mannheim, Germany) according to the manufacturer's protocol. Cells were grown on glass coverslips, fixed with 4% paraformaldehyde, and permeabilized with 0.1% Triton X-100 in 0.1% sodium citrate for 2 minutes on ice. Cells were incubated in TUNEL reaction mixture at 37°C for 60 minutes in a humidified dark chamber. The TUNEL-labeled samples were subjected to costaining with troponin-T antibodies for confirmation of cardiac identity. Coverslips were mounted onto glycerol-based mountant. Images were acquired using a Carl Zeiss fluorescence microscope with AxioVision 6.0 software (Zeiss GmbH, Gottingen, Germany). The number of apoptotic cells on electrical stimulation was further quantified using the APO-BrdU TUNEL Assay Kit (Molecular Probes, Inc, Eugene, OR). The dissociated cells were fixed in 1% (w/v) paraformaldehyde on ice for 15 minutes and then washed twice with Dulbecco phosphate-buffered saline at 300*g* for 5 minutes. The fixed cells were stored in ice-cold 70% (v/v) ethanol at −20°C before the nicked end labeling reaction. The cells were washed with wash buffer before incubation in TUNEL labeling solution for an hour at 37°C (10 μL reaction buffer, 0.75 μL TdT enzyme, 8 μL of BrdU, and 31.25 μL dH_2O). After further washing with rinse buffer, cells were

stained with the Alexa Fluor® 488 dye-labeled anti-BrdU antibodies for a half-hour. The propidium iodide/RNase A staining buffer was finally added to the cells before flow cytometry analysis. The positively labeled cells (green signal), a population with DNA fragmentation, were counted as percentage of apoptotic cells.

Taqman Assay for Quantification of *LMNA* Expression

Total RNA was extracted from fibroblasts using TRIZOL reagent following the procedure provided by the manufacturer (Life Technologies, Carlsbad, CA). For each sample, 1 μg of total RNA was used for cDNA synthesis using the QuantiTect Reverse Transcription kit (Qiagen, Venlo, The Netherlands). *Taqman* gene expression assay was carried out using a FAM-labeled probe derived from the Universal Probe Library (lamin A/C (*LMNA):* probe #66, troponin-T type 2 (*TNNT2*): probe #63 and α-tubulin (*TUB4q*): probe #75 (Roche Applied Sciences) in combination with FastStart Universal Probe Master (Rox) as the detection reagent (Roche Applied Sciences, Indianapolis, IN). The samples were analyzed as duplicates on the StepOnePlus real-time polymerase chain reaction system (Life Technologies). *TUBA4A* served as a housekeeping gene for normalization, and *TNNT2* was used for normalization of cardiac purity within the whole population.

Excitation-Contraction Coupling Analysis by Simultaneous Calcium Imaging and Video Edge Detection

To study the calcium-handling properties, hiPSC-derived cardiomyocytes were loaded with Fura-2 AM (Life Technologies, Carlsbad, CA), a calcium indicator, at a working concentration of 1 μM for 20 minutes. Unincorporated dye was removed, and the cells were subsequently incubated in Tyrode solution. For calcium transient measurements, field-stimulated electrical pacing was induced by the Myopacer EP Field Stimulator (IonOptix, Westwood, MA) at 40 V cm^{-1}, 5-millisecond pulse duration at frequencies of 0.5 Hz, 1 Hz, 1.5 Hz, and 2 Hz. The calcium fluorescence and video-edging (contractile force) signal were simultaneously recorded by MyoCam-S (IonOptix) using IonWizard 6.4 version 2 software (IonOptix). The acquisition rate of calcium imaging was 100 points/s. The Fura-2 required dual-wavelength excitation at 340 nm and 380 nm, and the emission signals were recorded at 505 nm. The calcium level was presented as a ratio of 340/380 nm ($F_{340/380}$) and calibrated with amount of free calcium (nmol/L). The calcium transients of every cardiomyocyte were recorded with background subtraction.

Statistical Analysis

Continuous variables are expressed as mean±SEM. Statistical comparisons between 2 groups were performed using Student t test or nonparametric Mann-Whitney test (for $n<10$). For analysis involving more than 2 groups, 1-way ANOVA analysis was used. For posttest, Tukey analysis was used to compare all pairs of columns. A P value <0.05 was considered statistically significant.

Results

Patient Characteristics, Generation of *LMNA*-Mutation-Harboring hiPSCs, and Cardiac Differentiation

Two patients with nonsense *LMNA* mutations and 1 patient with a frame-shift mutation were recruited to the study. The first patient was a 49-year old Chinese man who initially presented with atrial fibrillation and complete atrioventricular block and required permanent cardiac pacemaker implantation. Two years later, he developed sustained ventricular tachyarrhythmia and heart failure with an impaired left ventricular ejection fraction of 35%. An automatic implantable cardioverter defibrillator was therefore implanted (Table). His family history was remarkable for complete atrioventricular block and sudden cardiac death. Sequencing of the *LMNA* gene revealed a heterozygous single-base exchange (672G→T) in exon 4, resulting in an R225X nonsense mutation

Table. Cardiac Manifestations in Affected Subjects Bearing *LMNA* Mutations

LMNA Mutations	Sex	Cardiac Manifestations (Age of Manifestation)				
		Complete Heart Block	AF	VT/VF	Dilated Cardiomyopathy	AICD
R225X	M	+ (49)	+ (49)	+ (50)	+ (51)	+ (52)
Q354X	M	+ (50)	+ (50)	+ (56)	+ (50)	+ (50)
T518fs	M	+ (43)	+ (43)	+ (47)	+ (47)	+ (47)

AF indicates atrial fibrillation; AICD, automatic implantable cardioverter defibrillator; VT/VF, ventricular tachycardia/ventricular fibrillation.
"+" represent presence of disease phenotype, while the ages of disease onset are shown the brackets.

(truncation in the coil 1B domain of both lamin A and C proteins), previously known to be associated with familial dilated cardiomyopathy[18,27,28] (Figure 1A and 1B). The second patient was a 50-year old Chinese man who also had atrial fibrillation, complete atrioventricular block, ventricular tachyarrhythmia, and heart failure. Of his 4 siblings, 3 had similar cardiac conditions, and all had had an automatic implantable cardioverter defibrillator implanted. A heterozygous single-base exchange (1062C→T) in exon 6 of the *LMNA* gene resulting in a Q354X nonsense mutation was found to be cosegregated with the cardiac phenotype in this family (Figure 1). The last patient was a 43-year-old Chinese man with atrial fibrillation, complete atrioventricular block, and ventricular tachyarrhythmia. A heterozygous single-base deletion (1554delC) at exon 9 of the *LMNA* gene was detected. According to our prediction of a second open reading frame with 1 "C" deletion at codon position 1554 in the *LMNA* mRNA transcript (NM_170707), the premature stop codon with sequence of "TGA" will be generated at an earlier position at the 547th amino acid, shortening the LMNA protein that is supposed to be transcribed (reduced from 665 to 547 amino acids) (Figure S1). This patient's paternal uncle

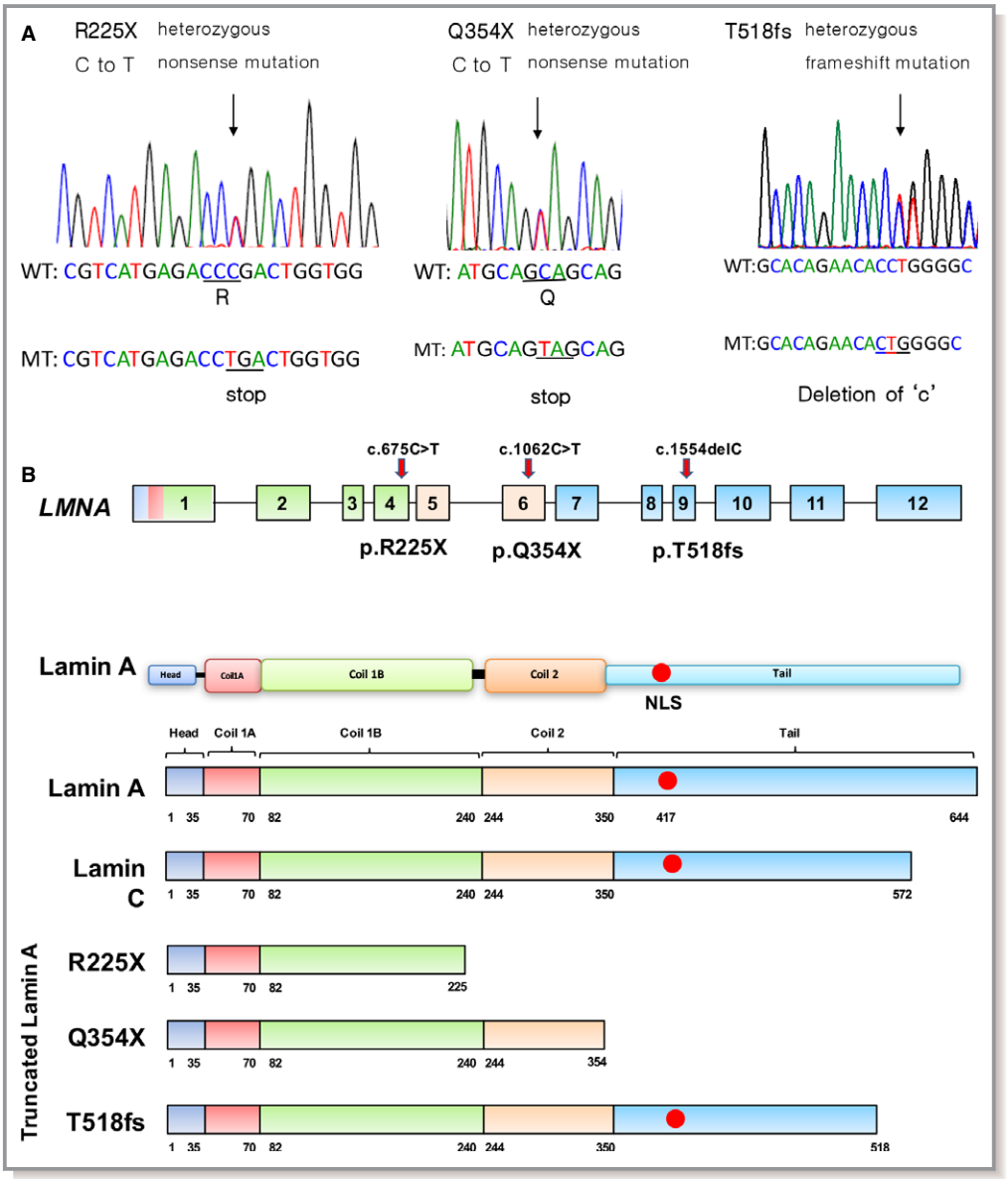

Figure 1. Schematic diagram illustrating the *LMNA* mutations involved in this study. A, Genetic disorders caused by nonsense and frame-shift mutations in *LMNA*. R225X yielded a premature stop codon, TGA, due to a C-to-T substitution; Q354X also yielded a premature stop codon, TAG, due to a C-to-T substitution; and the frameshift mutation T518fs resulted from a C deletion. B, Splice variant of *LMNA* gene yielding lamin A/C protein: the mutation yielded 3 different lengths of truncated lamin A/C protein. Key: NLS indicates nuclear localization signal.

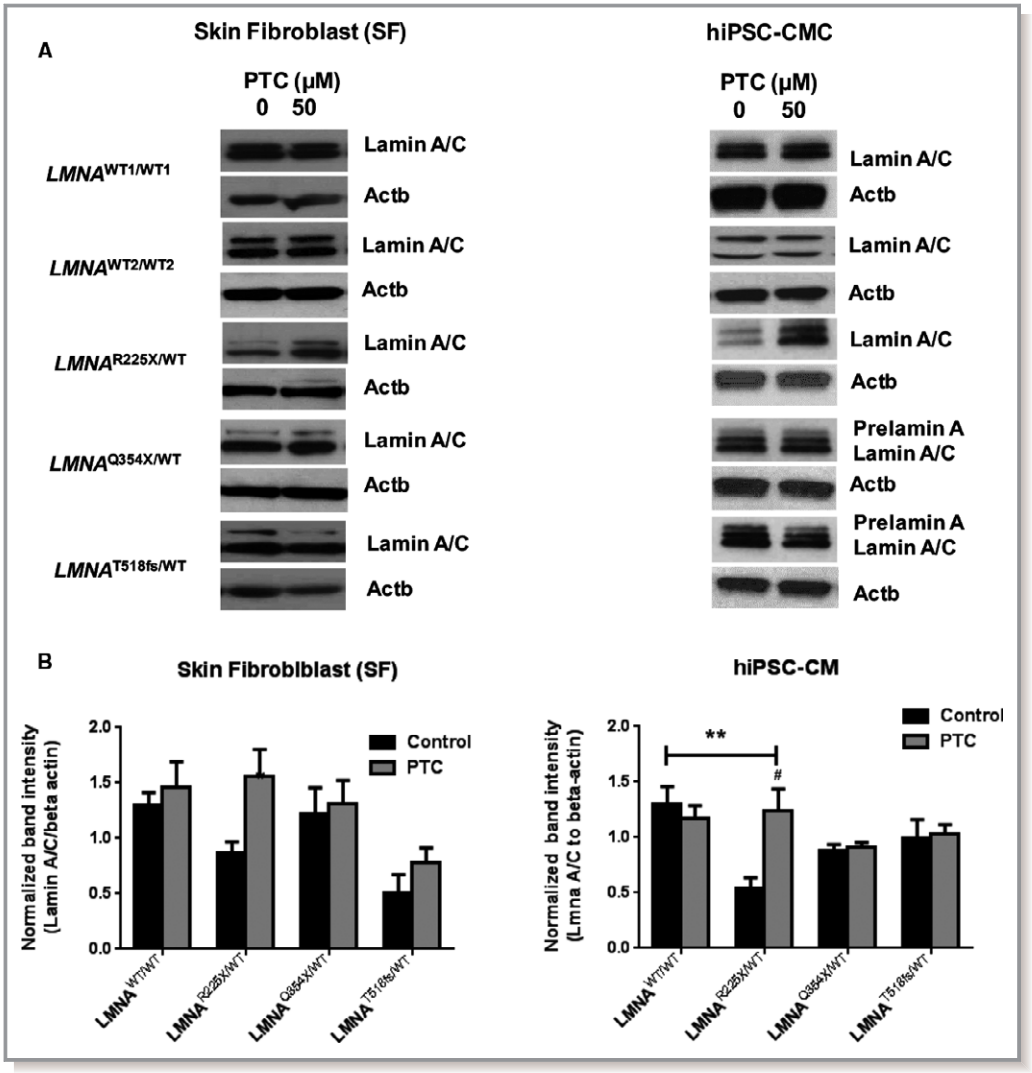

Figure 2. Effects of PTC124 on the expression of lamin A/C proteins in dermal fibroblasts and hiPSC-derived cardiomyocytes (hiPSC-CMC) derived from wild-type ($LMNA^{WT1/WT1}$ and $LMNA^{WT2/WT2}$) and *LMNA* mutants ($LMNA^{R225X/WT}$, $LMNA^{Q354X/WT}$, and $LMNA^{T518fs/WT}$). A, Representative immunoblot and (B) quantitative data of protein-normalized lamin A/C protein expression. The band intensities of lamin A/C and β-actin (Actb) were measured from the high-resolution (300×300 dots per inch) images using Image J. At least 3 to 6 independent samples were prepared for Western blot analysis. The significant difference of quantitative data was tested by 2-way ANOVA with post hoc Turkey multiple comparison test (**$P<0.01$ as indicated by arrows; #$P<0.05$, Control vs PTC). Original images of immunoblots in individual experiments are shown in Figure S2. hiPSC indicates human induced pluripotent stem cells.

had had atrial fibrillation and complete atrioventricular block (Figure 1A and 1B). Dermal fibroblasts were obtained from these patients during automatic implantable cardioverter defibrillator implantation, and patient-specific hiPSCs harboring the specific mutations were generated accordingly. The patient-specific *LMNA* mutations in these hiPSCs had been confirmed by genomic DNA sequencing analysis. For simplicity in description, the hiPSC lines containing the 672G→T, 1062C→T, and 1554delC mutations in 1 of the *LMNA* alleles will be denoted as R225X, Q354X, and T518fs mutants, respectively, in this article.

The commercially available hiPSC line (line IMR90, WicellI) and KS1 hiPSC line generated by our lab by lentiviral reprogramming that do not contain any *LMNA* mutations was used as a wild-type control in this study [21] (Figure 1).

Effects of PTC124 on Expression of Lamin A/C Proteins in Dermal Fibroblasts and hiPSC-Derived Cardiomyocytes

First, we tested the effects of PTC124 on the level of lamin A/C proteins in dermal fibroblasts obtained from the 3 patients

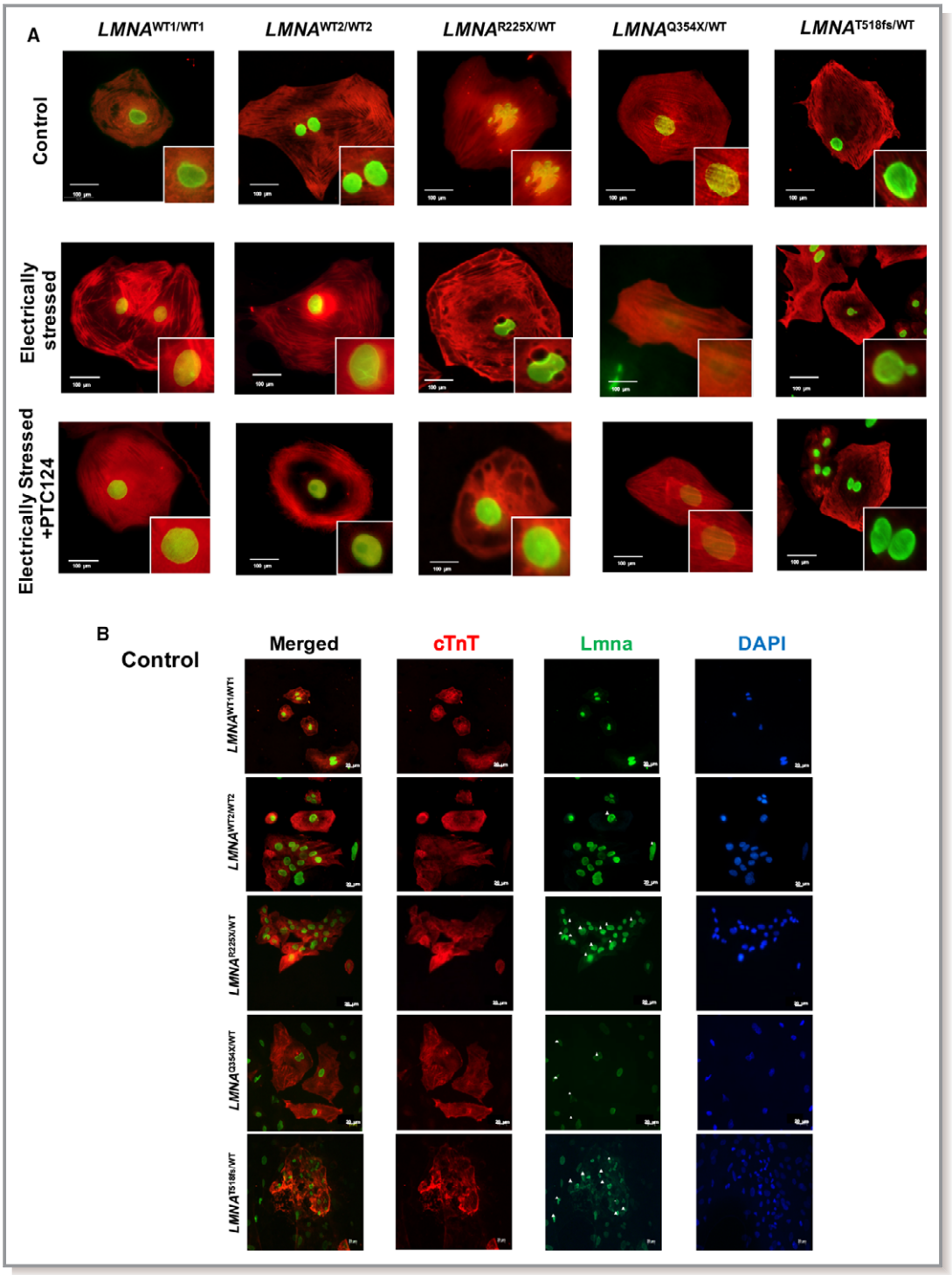

Figure 3. Nuclear blebbing in the hiPSC-derived cardiomyocytes. The 2 wild-type lines (*LMNA*$^{WT1/WT1}$ and *LMNA*$^{WT2/WT2}$), R225X (*LMNA*$^{R225X/WT}$), Q354X (*LMNA*$^{Q354/WT}$), and T518fs (*LMNA*$^{T518fs/WT}$), mutant hiPSC lines were differentiated into cardiomyocytes and treated with PTC124. The occurrence of cardiac nuclear blebbing was revealed with coimmunostaining of cardiac troponin T (red) and lamin A/C (green). A, A single representative hiPSC CMC, and (B through D) representative images of lower magnification were used to quantify the portion of nuclear blebbing in a single field. At least 3 countings were performed. E, Quantitative data of nuclear blebbing count. The significant difference of quantitative data was tested by 2-way ANOVA with post hoc Turkey multiple comparison test ($^{***}P<0.0001$ as indicated by arrows; $^{\#\#\#\#}P<0.0001$ control vs treatment group). cTnT indicates cardiac troponin-T; DAPI, 4,6-diamidino-2-phenylindole dihydrochloride; hiPSC, human induced pluripotent stem cells; LMNA, lamin.

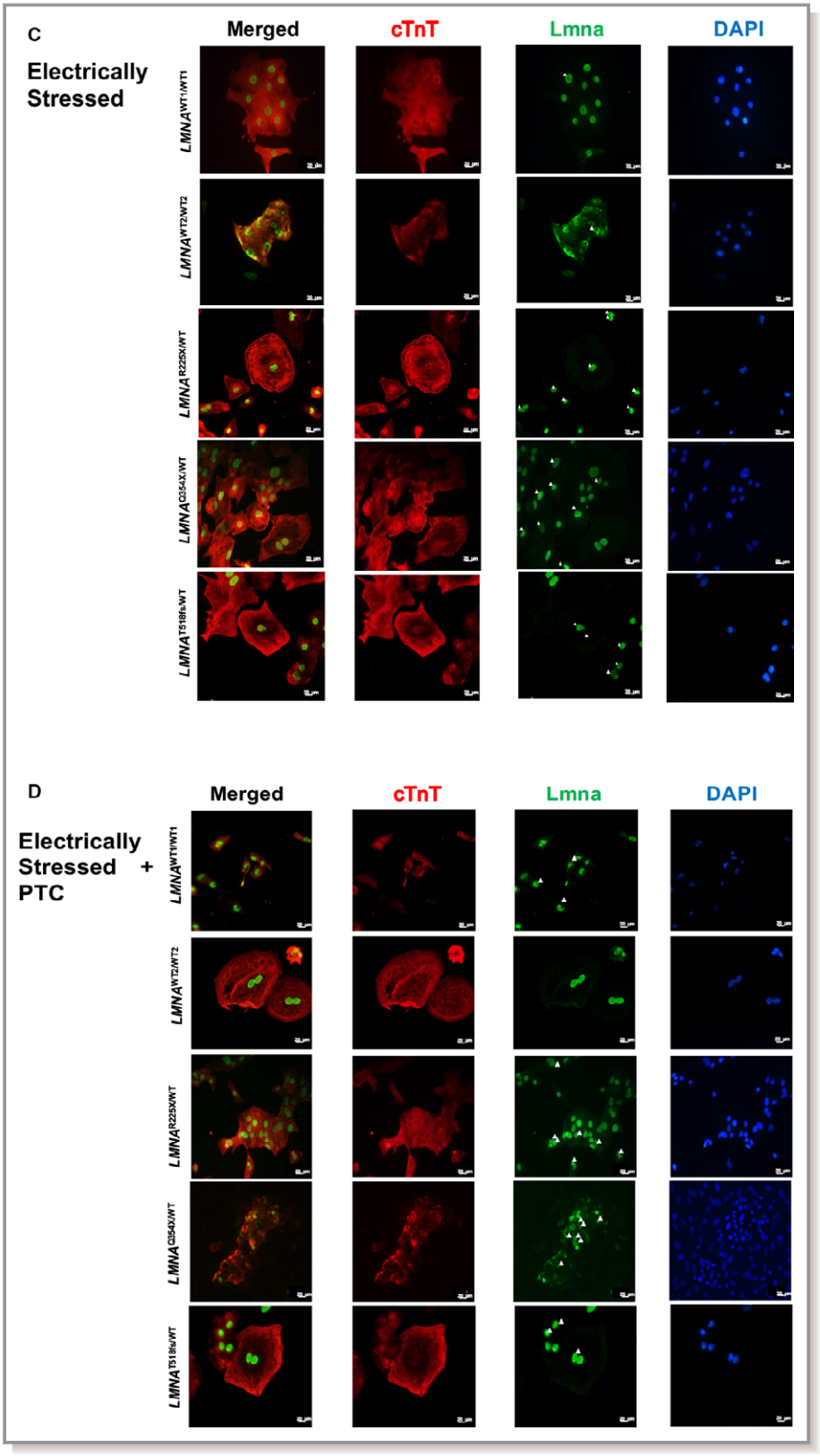

Figure 3. Continued

with *LMNA*-related cardiomyopathy (Figure 2). Dermal fibroblasts were treated with PTC124 (50 μmol/L), and the lamin A/C protein levels were evaluated by Western blotting analysis. In the absence of PTC124, the translation yielded only intact lamin A/C products: a 74-kDa band indicating lamin *A* protein and a 63-kDa band from lamin C protein, in

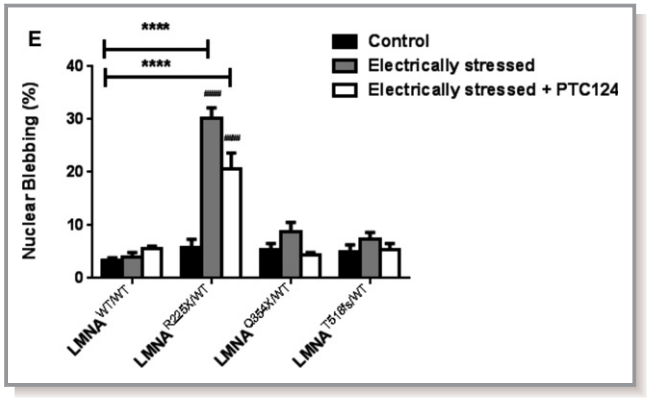

Figure 3. Continued

dermal fibroblasts from all 3 patients. No truncated lamin A/C protein was detected in any of the mutant lines (data not shown) (Figure 2). Compared with their wild-type counterpart, the levels of lamin A/C proteins were markedly reduced in dermal fibroblasts from all mutant lines. Treatment with PTC124 increased the level of both lamin A and C isoforms in dermal fibroblasts carrying the R225X mutation in the *LMNA* gene but not in the wild-type or dermal fibroblasts from the other 2 patients harboring Q354X or T518fs mutations. Importantly, as no prolonged lamin A/C protein products were detected, PTC124 treatment was not likely causing normal termination codon read-through.

Similar results were observed in the hiPSC-derived cardiomyocytes treated with PTC124. In brief, the level of lamin A/C proteins in all 3 mutant lines was substantially reduced compared with their wild-type counterpart in the absence of PTC124 (Figure 2). Similar to the findings observed in dermal fibroblasts, PTC124 treatment increased the level of both lamin A and C proteins in cardiomyocytes derived from the R225X mutant hiPSC line but not in those of the other 2 *LMNA* mutations (ie, Q354X and T518fs mutants). Interestingly, mild accumulation of prelamin A was observed in the cardiomyocytes derived from Q354X and T518fs mutants (Figure 2), regardless of the presence of PTC124 treatment.

Effects of PTC124 on Electrical Stimulation–Induced Nuclear Senescence and Apoptosis in hiPSC-Derived Cardiomyocytes

As previously reported by our team[18] and others,[29] the nuclei of cardiomyocytes from *LMNA*-related cardiomyopathy often exhibit dysmorphic features such as micronucleation (blebbing), one of the hallmarks of nuclear senescence.[30] These changes together with apoptosis are often exaggerated in cardiomyocytes that are electrically active[29] or under constant electrical stress.[18] As shown in Figure 3, coimmunostaining of lamin A/C (green) and cardiac troponin-T (red) revealed that the cardiomyocytes derived from R225X or T518fs mutant lines exhibited nuclear blebbing even in the absence of external stress. After continuous electrical stressing, the nuclear blebbing events became more frequent in all the hiPSC-derived cardiomyocytes carrying *LMNA* mutations. Interestingly, the application of PTC124 alleviated nuclear senescent morphological abnormalities in the cardiomyocytes derived from the R225X mutant but not in those derived from the Q354X or T518fs mutant lines (Figure 3A through 3D). To evaluate the effects of PTC124 on apoptosis, we first performed TUNEL analysis. As shown in Figure 4A through 4D, in concordance with the nuclear blebbing assay, the electrical stress-induced apoptosis in cardiomyocytes with R225X mutation was markedly reduced in the presence of PTC124 (Figure 4B). Nonetheless, no significant changes in apoptosis were detected on application of PTC124 in the other 2 mutants (Figure 4C through 4D). In order to provide more quantitative assessment of the protective effects of PTC124 against electrical stress-induced apoptosis, we further quantified the proportion of apoptotic cells using the APO-BrdU TUNEL assay (Figure 4F through 4G and Table S1). Compared with the wild-type control, all 3 mutants showed a significantly higher proportion of apoptotic cardiomyocytes. On electrical stressing, the proportion of apoptotic cells increased markedly by 40.58% (n=3-7, $P<0.05$) only in hiPSC-derived cardiomyocytes with the R225X mutation (Figure 4G). More importantly, application of PTC124 significantly reduced the electrical stimulation-induced apoptotic population by 41.89% in cardiomyocytes derived from R225X mutant (n=3-5; $P<0.05$). Neither electrical stress nor the application of PTC124 caused any statistically significant changes to the proportion of apoptotic cells in any of the other groups.

Nonsense *LMNA* mRNA Degradation

In addition to defective translation as a result of the nonsense mutations, the suppressed production of lamin

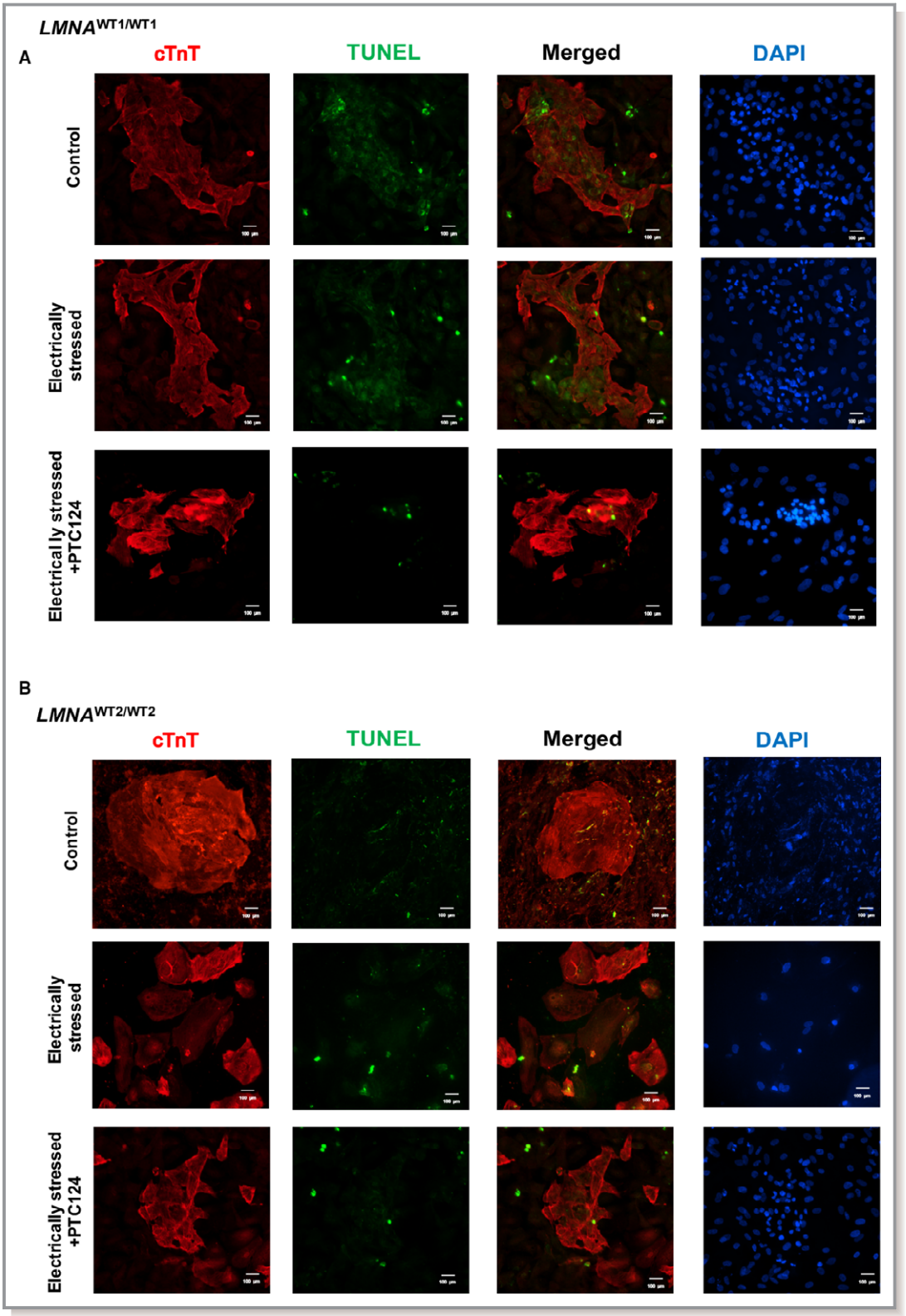

Figure 4. Evaluation of TUNEL-positive apoptotic cell in electrically stressed and PTC124-treated cardiomyocytes derived from wild-type (*LMNA*$^{WT1/WT1}$ and *LMNA*$^{WT2/WT2}$) and *LMNA* mutants (*LMNA*$^{R225X/WT}$, *LMNA*$^{Q354X/WT}$, and *LMNA*$^{T518fs/WT}$) by (A through E) immunostaining; (F through G) and also by Apo-BrdU TUNEL-FACS analysis to quantify apoptotic cells (Significant difference was analyzed by 2-way ANOVA with Tukey multiple comparison post-hoc test $^{*}P<0.05$; n=3 to 5 (as indicted by arrows) and (control vs electrically stressed) $^{\#}P<0.05$; n=3 to 7). FACS indicates fluorescence-activated cell sorting; TUNEL, terminal deoxynucleotidyl transferase dUTP nick end labeling.

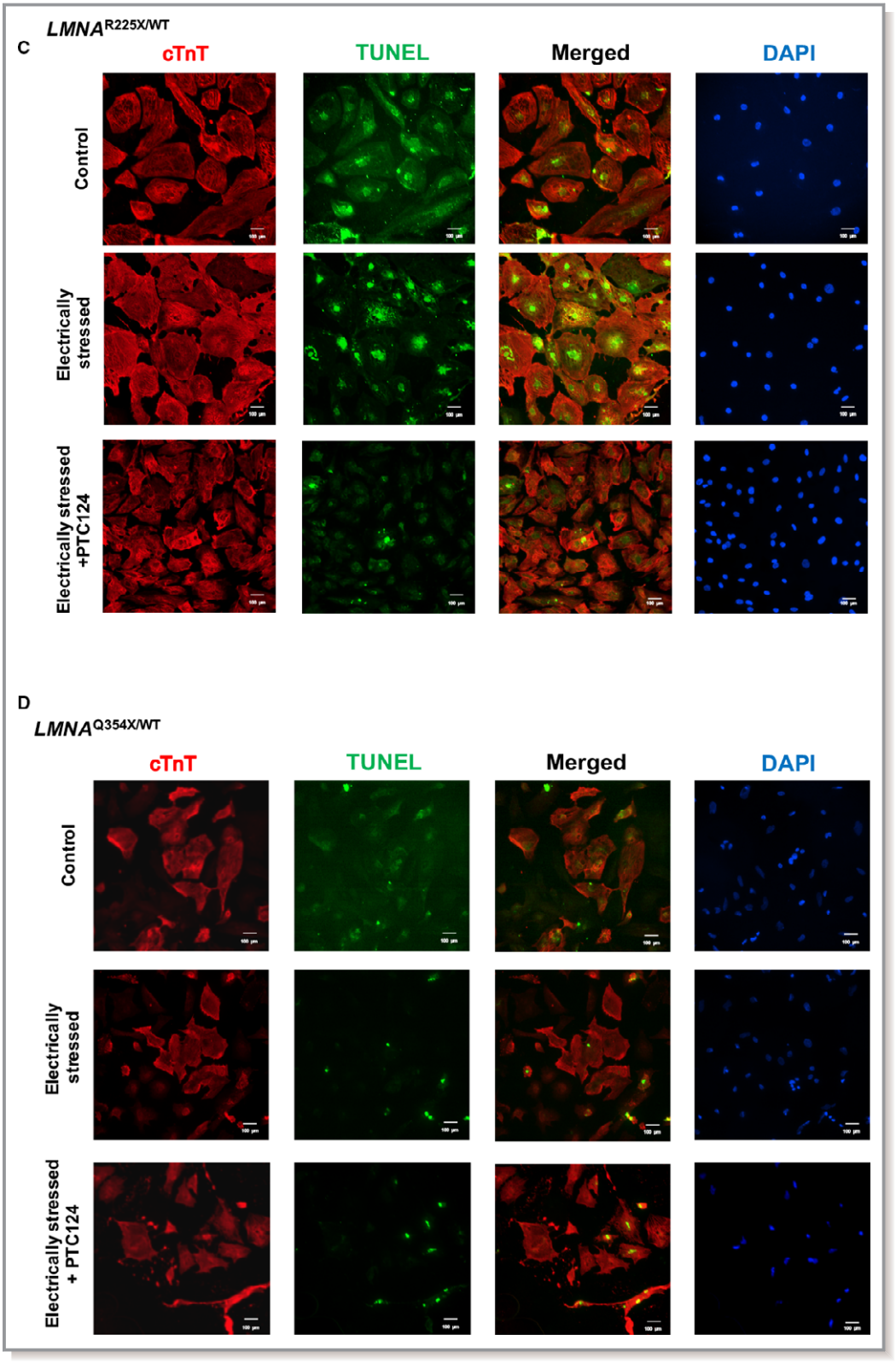

Figure 4. Continued

A/C proteins could be due to a nonsense-mediated mRNA decay mechanism.[31] To evaluate such a possibility, we precisely quantified the *LMNA* mRNA level in cardiomyocytes derived from the wild-type and mutant lines using *Taqman* real-time polymerase chain reaction assay. As shown in Figure 5, the relative cardiac *LMNA* expression in all 3

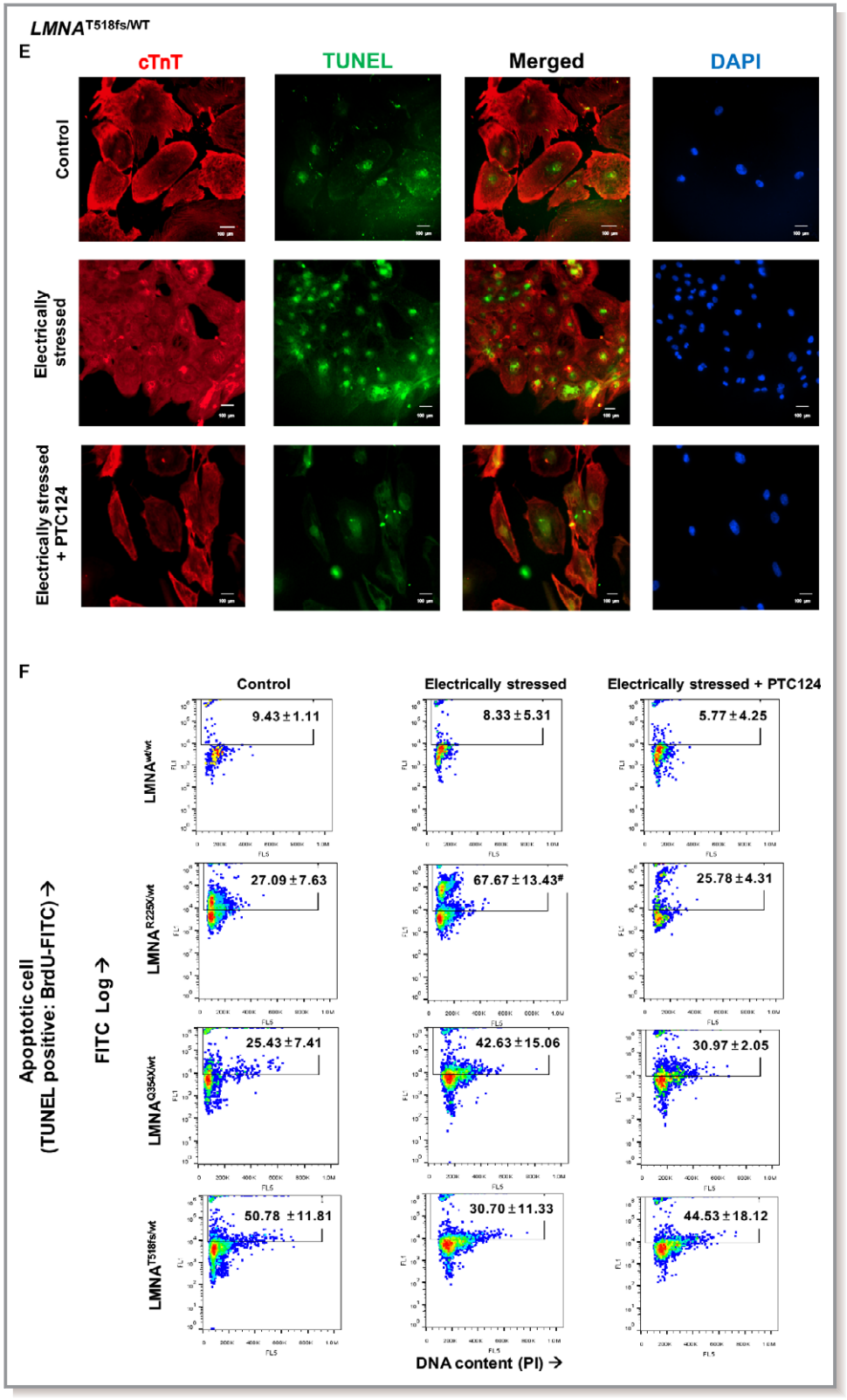

Figure 4. Continued

mutants was significantly lower than that in the wild-type control. This suggests that nonsense mRNA degradation may contribute to the reduced lamin A/C protein level. Interestingly, PTC124 could not restore the mRNA production in any mutant line, suggesting that its activity was limited to a translational level.

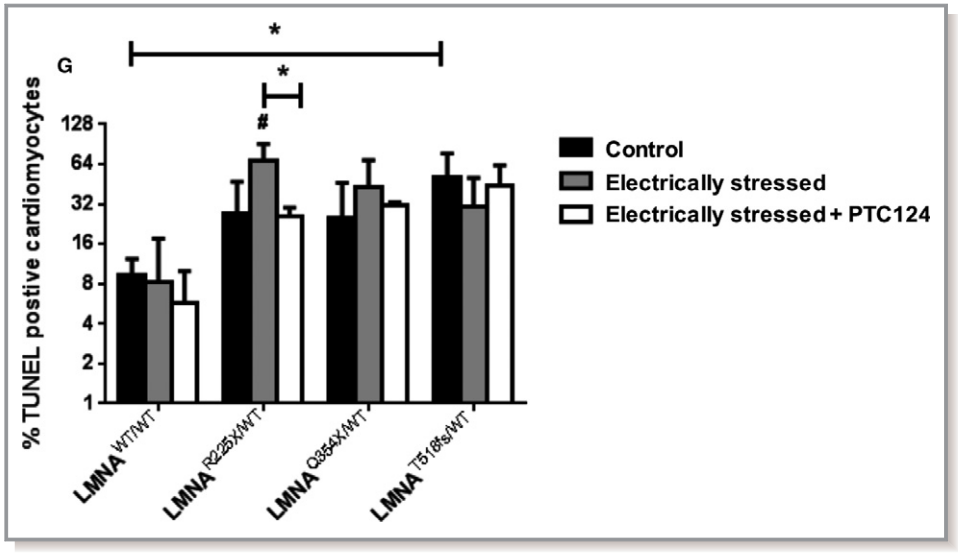

Figure 4. Continued

Effects of PTC124 on Excitation-Contraction Coupling in Cardiomyocytes Derived From the R225X Mutant hiPSC

Because the PTC124-mediated reduction in apoptosis was observed only in the cardiomyocytes derived from the R225X mutant and not in other lines, we further evaluated the effects of PTC124 on excitation-contraction coupling, calcium homeostasis, and contractile abnormalities in this particular line. Contractilities and calcium transients were recorded simultaneously under field electrical pacing at frequencies ranging from 0.5 Hz to 2 Hz. As shown in Figure 6A, hiPSC-derived cardiomyocytes (both wild-type and mutants) were responsive to electrical pacing and showed comparable diastolic and peak calcium levels (Figure 6B and 6D). Diastolic calcium levels (indicated by the baseline levels of the calcium transient tracings) of both lines increased as the pacing frequency increased (Figure 6B). In general, the maximum calcium released (indicated by the peak amplitude of the calcium transient tracings) in cardiomyocytes derived from the R225X mutant was less than that released in the wild-type counterparts (Figure 6C). The systolic cell length also reduced remarkably in the mutant cardiomyocytes treated with PTC124, indicating a more efficient coupling between intracellular calcium surge and cellular contraction (Figure 6E). Regardless of the application of PTC124, there was no significant change in the upstroke velocity (ie, the rate of calcium release) of calcium transients or rate of cell shortening between wild-type and mutant hiPSC-derived cardiomyocytes (Figure 6F and 6G). Nevertheless, at high pacing speed (2 Hz), PTC124 significantly improved the rate of calcium reuptake in the mutant cardiomyocytes (as indicated by a more negative value of V_{max} decay) ($P<0.05$, n=3) (Figure 6H). Furthermore, PTC124 treatment appeared to improve the rate of cellular relengthening in the mutant cardiomyocytes (Figure 6I).

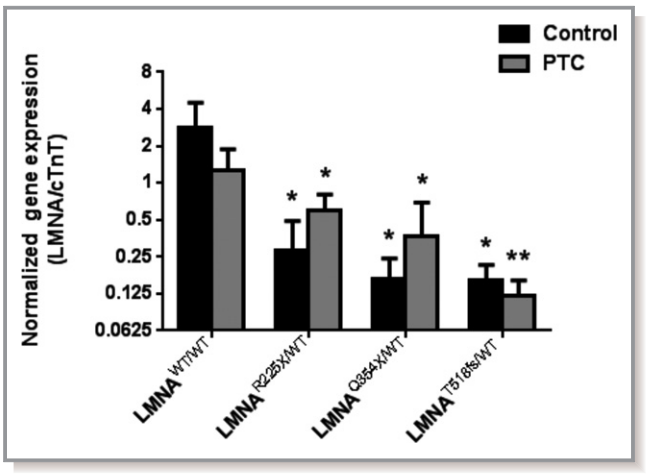

Figure 5. Normalized gene expression level of *LMNA* in PTC124-treated hiPSC-derived cardiomyocytes. The endogenous control gene was *TUBB,* and *TNNT2* was used to normalize the number of cardiac cells within the differentiated population. Significant difference was analyzed by 1-way ANOVA with Tukey multiple comparison post hoc test compared with wild-type control group, *$P<0.05$ and **$P<0.01$; n=5. hiPSC indicates human induced pluripotent stem cells.

Discussion

Precision medicine, according to the National Institutes of Health in the United States, is an emerging approach for disease treatment and prevention that takes into account

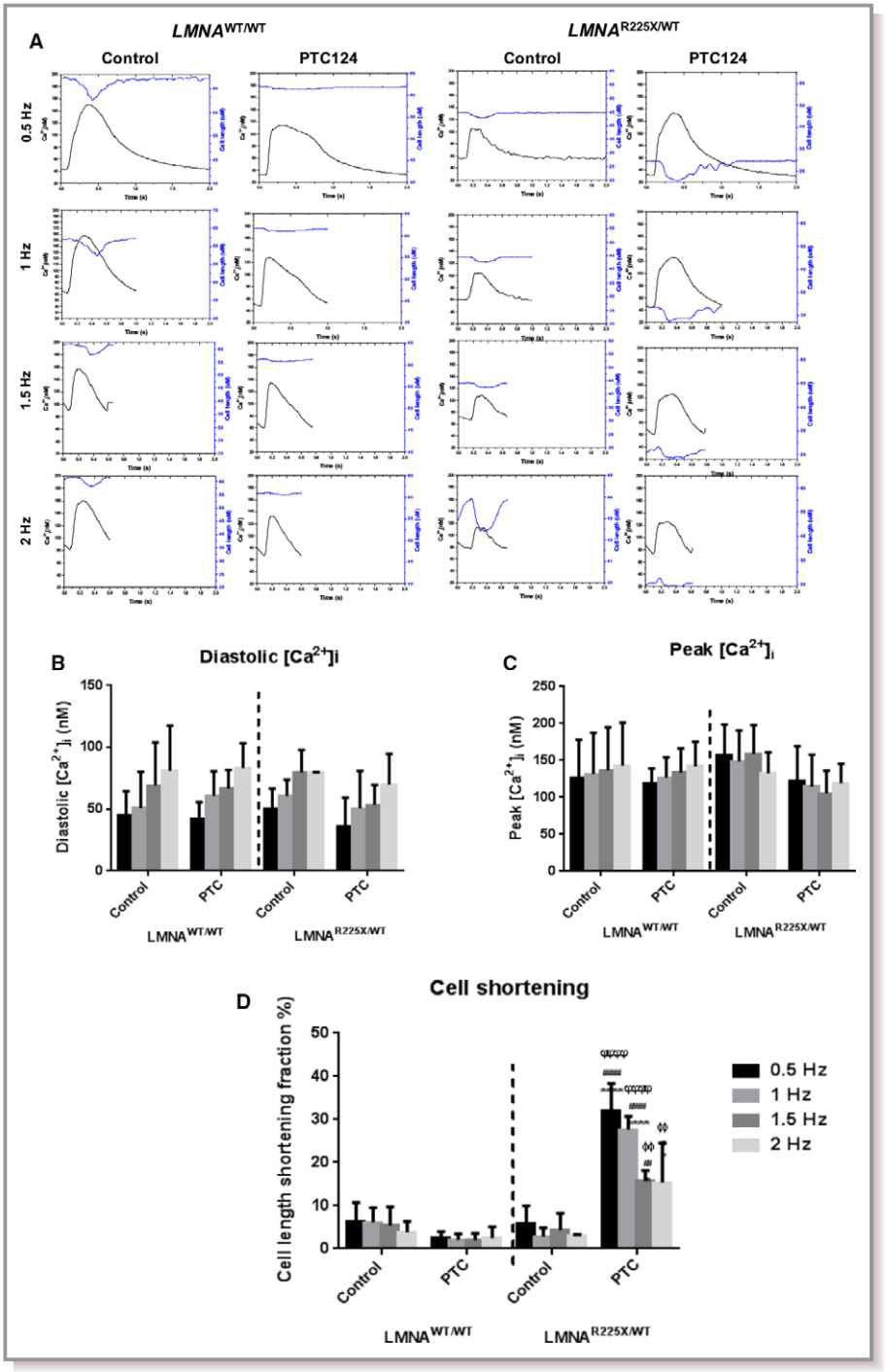

Figure 6. Excitation-contraction (EC) coupling was improved by PTC124 in the cardiomyocytes derived from the R255X mutant. A, Representative tracing of calcium transient and cell-shortening in *LMNA*$^{WT/WT}$ and *LMNA*$^{R225X/WT}$ cells treated with PTC124. Rate dependence of calcium transients and cell contractility pacing frequency range of 0.5, 1, and 1.5 to 2 Hz are shown in terms of (B) diastolic calcium, (C) peak calcium amplitude, (D) fractional shortening (%) (**P*<0.05; n=5 to 7; WT: PTC vs R225X:PTC $^{\#\#\#\#}$*P*<0.0001; R225X: 0.5-Hz control vs R225X: 0.5-Hz or 1-Hz PTC: φ φ φ φ *P*<0.0001; R225X: 0.5 Hz PTC vs R225X: 1.5 or 2 Hz PTC: φ φ *P*<0.001); (E and F) maximal upstroke velocity (V_{max} upstroke) of calcium transient and rate of cell shortening (ie, contraction); (G and H) maximal decay velocity (V_{max} decay) and rate of cell relengthening (ie relaxation). Improved calcium decay kinetics and relaxation performance are shown (G and H). Significant difference was analyzed by comparing pacing rate of 0.5 Hz with the other rates of the same treatment group in 1 cell line, or otherwise indicated by arrows using 2-way ANOVA with Turkey test as post hoc (**P*<0.05).

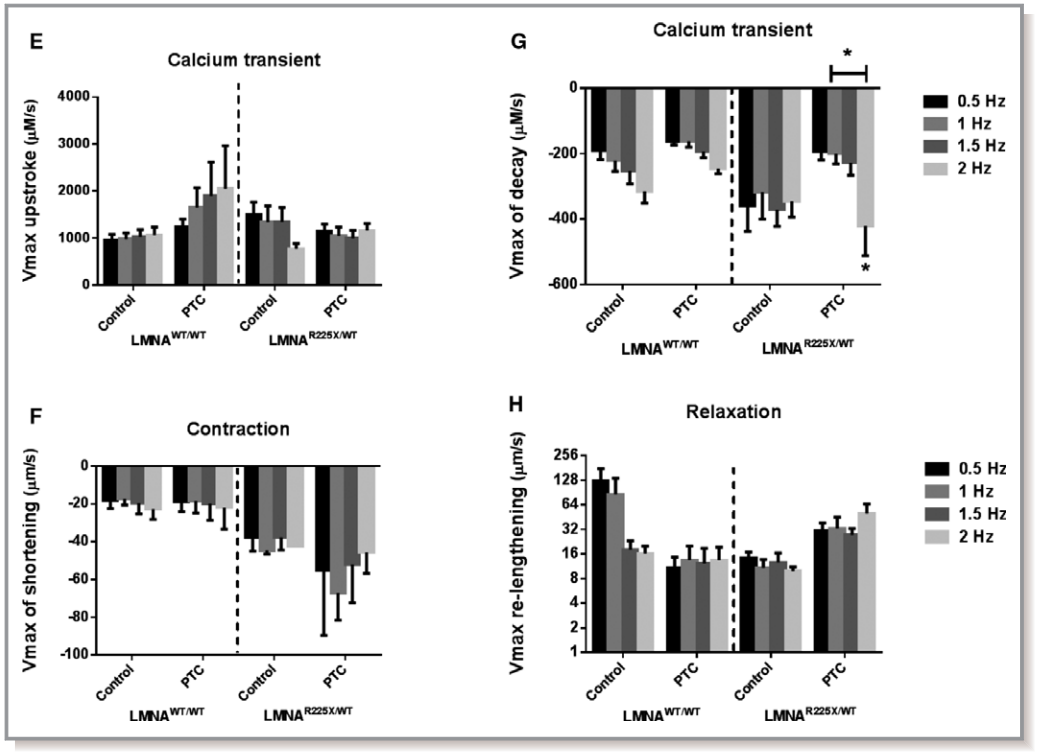

Figure 6. Continued

individual variability in environment, lifestyle, and genetic makeup for individual patients.[32,33] The assumption is that differences in an individual patient's genetic makeup as well as environmental factors contribute to his or her differential clinical outcome, particularly in responsiveness to treatments. In other words, patients with apparently similar clinical conditions may be treated differently because of these individual differences. Over the past 3 decades, there has been tremendous progress in genetics research that has identified numerous genes responsible for dilated cardiomyopathies and provided novel insight into their pathogenic mechanisms. Nonetheless, translation of these research findings to clinical practice remains incomplete. In fact, even with the availability of an individual patient's genetic information that underlies dilated cardiomyopathies, a disease-specific intervention designed to tackle the root causes of the condition is rarely available. As a result, despite different genetic etiologies and pathogeneses, dilated cardiomyopathies are often treated similarly simply based on clinical presentations.

Mutations in *LMNA* genes are the most common cause of familial dilated cardiomyopathy, particularly among those with concomitant atrioventricular conduction block.[7,8] In our study, despite different mutations in the 3 patients with *LMNA*-related cardiomyopathy, their clinical presentations were remarkably similar with early onset atrioventricular block and atrial fibrillation around the fourth decade of life, followed by ventricular tachyarrhythmia and heart failure in the fifth to sixth decade of life. The condition was inherited in an autosomal dominant pattern in all 3 families. In accordance with their genotypes, both dermal fibroblasts and cardiomyocytes derived from R225X, Q354X, and T518fs mutants displayed reduced lamin A/C protein production. As demonstrated in our previous hiPSC-based model of *LMNA*-related cardiomyopathy,[18] cardiomyocytes derived from these 3 mutants exhibited nuclear senescence and apoptosis that were aggravated in the presence of electrical stress. Nonetheless, despite their very similar clinical presentations and cellular phenotypes, there was a differential effect of PTC124 on lamin A/C protein production in their primary dermal fibroblasts (R225X>>Q354X and T518fs). Similar to dermal fibroblasts, PTC124 restored lamin A/C protein production only in cardiomyocytes derived from the R225X mutants but not in their Q354X or T518fs counterparts. More importantly, the increase in lamin A/C production was associated with alleviated nuclear senescence and reduced apoptosis. Furthermore, PTC124 treatment improved the excitation-contraction coupling and contractile functions of the hiPSC-derived cardiomyocytes carrying the R225X mutation.

The lack of responsiveness to PTC124 of cardiomyocytes derived from the T518fs mutant, which served as a negative control, is expected. On the contrary, for the cardiomyocytes derived from the Q354X mutant, the lack of efficiency could be explained by the difference in nucleotide sequence of the mutant premature stop codons. Nonsense mutations are

point mutations that result in the occurrence of 1 of 3 stop codons, UAG, UAA, or UGA, in the messenger RNA coding region, leading to a truncated protein product due to premature termination of mRNA translation and/or promotion of mRNA destabilization by nonsense-mediated mRNA decay. Although PTC124 promotes read-through of all 3 nonsense codons, its potency differs according to the nucleotide sequences of the premature stop codons, with the highest read-through at UGA, followed by UAG, and then UAA.[10] For the 2 nonsense mutations, the R225X mutation in the *LMNA* gene is a result of a premature stop codon (UGA) that is the most PTC124-responsive nucleotide sequence, whereas in the Q354X mutant, the sequence of the stop codon is UAG, which seems to be less PTC124 responsive. Because the efficacy of the translational read-through of premature stop codons and production of full-length proteins by interfering with ribosomal proofreading depend on the availability of nonsense transcripts to the ribosomal translational machinery, it is interesting that in our study, application of PTC124 increased mRNA expression of the 2 nonsense transcripts: R225X and Q354X. Nonetheless, it is beyond the scope of the present study to determine whether PTC124 can affect the efficiency of the nonsense mutation mRNA decay mechanisms.

For nonsense mutation, it seems to be stating the obvious that translational read-through of premature stop codons with PTC124 is expected to produce full-length proteins and reverse the pathogenic process. Nonetheless, in a recent study using hiPSC-derived cardiomyocytes from 2 patients who harbored nonsense mutations in the sodium channel gene *SCN5A*, R1638X and W156X, although the premature stop codon sequences in both mutations were the most optimum sequence for PTC124, UGA, PTC124 and gentamicin, another premature stop codon read-through agent, failed to restore sodium current I_{Na}.[34] Although the sodium channel protein level was not quantified to document the restored protein translation, other downstream mechanisms such as a trafficking defect might have been responsible. This reinforces the need for precision medicine. hiPSC technology and in vitro drug testing strategies provide unparalleled opportunities to realize the promise of precision medicine. This strategy may be exploited to select the patients with maximum drug responsiveness for standard clinical trials. Then, the expected drug effects may be much larger, and the required sample size would then be much smaller, making standard randomized clinical trials possible.

Conclusions

Taken collectively, PTC124 promoted translation read-through of premature stop codons in patient-specific hiPSC-derived cardiomyocytes that harbored the mutation R225X in the *LMNA* gene and alleviated nuclear senescence, apoptosis, and altered excitation-contraction coupling. The same effects were not evident in patient-specific hiPSC-derived cardiomyocytes that harbored another nonsense mutation or a frame-shift mutation. Based on our data, hiPSC technology represents a general approach to predict the clinical response of patients with an apparently similar clinical condition and to realize the potential of precision medicine.

Acknowledgments

We are thankful for the technical support provided by Dr Au.

Disclosures

None.

References

1. Lin F, Worman HJ. Structural organization of the human gene encoding nuclear lamin A and nuclear lamin C. *J Biol Chem*. 1993;268:16321–16326.
2. Capell BC, Collins FS. Human laminopathies: nuclei gone genetically awry. *Nat Rev*. 2006;7:940–952.
3. Burke B, Stewart CL. The laminopathies: the functional architecture of the nucleus and its contribution to disease. *Annu Rev Genomics Hum Genet*. 2006;7:369–405.
4. Dreesen O, Stewart CL. Accelerated aging syndromes, are they relevant to normal human aging? *Aging*. 2011;3:889–895.
5. Rankin J, Ellard S. The laminopathies: a clinical review. *Clin Genet*. 2006;70:261–274.
6. Worman HJ, Fong LG, Muchir A, Young SG. Laminopathies and the long strange trip from basic cell biology to therapy. *J Clin Invest*. 2009;119:1825–1836.
7. Fatkin D, Otway R, Richmond Z. Genetics of dilated cardiomyopathy. *Heart Fail Clin*. 2010;6:129–140.
8. Dellefave L, McNally EM. The genetics of dilated cardiomyopathy. *Curr Opin Cardiol*. 2010;25:198–204.
9. Wolf CM, Wang L, Alcalai R, Pizard A, Burgon PG, Ahmad F, Sherwood M, Branco DM, Wakimoto H, Fishman GI, See V, Stewart CL, Conner DA, Berul CI, Seidman CE, Seidman JG. Lamin a/c haploinsufficiency causes dilated cardiomyopathy and apoptosis-triggered cardiac conduction system disease. *J of mol and cell cardiol*. 2008;44:293–303.
10. Welch EM, Barton ER, Zhuo J, Tomizawa Y, Friesen WJ, Trifillis P, Paushkin S, Patel M, Trotta CR, Hwang S, Wilde RG, Karp G, Takasugi J, Chen G, Jones S, Ren H, Moon YC, Corson D, Turpoff AA, Campbell JA, Conn MM, Khan A, Almstead NG, Hedrick J, Mollin A, Risher N, Weetall M, Yeh S, Branstrom AA, Colacino JM, Babiak J, Ju WD, Hirawat S, Northcutt VJ, Miller LL, Spatrick P, He F, Kawana M, Feng H, Jacobson A, Peltz SW, Sweeney HL. Ptc124 targets genetic disorders caused by nonsense mutations. *Nature*. 2007;447:87–91.
11. Du M, Liu X, Welch EM, Hirawat S, Peltz SW, Bedwell DM. Ptc124 is an orally bioavailable compound that promotes suppression of the human CFTR-G542X nonsense allele in a CF mouse model. *Proc Natl Acad Sci USA*. 2008;105:2064–2069.
12. Hirawat S, Welch EM, Elfring GL, Northcutt VJ, Paushkin S, Hwang S, Leonard EM, Almstead NG, Ju W, Peltz SW, Miller LL. Safety, tolerability, and pharmacokinetics of PTC124, a nonaminoglycoside nonsense mutation suppressor, following single- and multiple-dose administration to healthy male and female adult volunteers. *J Clin Pharmacol*. 2007;47:430–444.
13. Clinicaltrials.gov. A phase 3 efficacy and safety study of ataluren (PTC124®) in patients with nonsense mutation cystic fibrosis. https://clinicaltrials.gov/ct2/show/study/NCT02139306. Accessed January 1, 2017.
14. Tse HF, Ho JC, Choi SW, Lee YK, Butler AW, Ng KM, Siu CW, Simpson MA, Lai WH, Chan YC, Au KW, Zhang J, Lay KW, Esteban MA, Nicholls JM, Colman A, Sham PC. Patient-specific induced-pluripotent stem cells-derived cardiomyocytes recapitulate the pathogenic phenotypes of dilated cardiomyopathy due to a novel DES mutation identified by whole exome sequencing. *Hum Mol Genet*. 2013;22:1395–1403.

15. Ng KM, Mok PY, Butler AW, Ho JC, Choi SW, Lee YK, Lai WH, Au KW, Lau YM, Wong LY, Esteban MA, Siu CW, Sham PC, Colman A, Tse HF. Amelioration of X-linked related autophagy failure in Danon disease with DNA methylation inhibitor. *Circulation*. 2016;134:1373–1389.
16. Lee YK, Lau YM, Ng KM, Lai WH, Ho SL, Tse HF, Siu CW, Ho PW. Efficient attenuation of Friedreich's ataxia (FRDA) cardiomyopathy by modulation of iron homeostasis—human induced pluripotent stem cell (hiPSC) as a drug screening platform for FRDA. *Int J Cardiol*. 2016;203:964–971.
17. Ho JC, Zhou T, Lai WH, Huang Y, Chan YC, Li X, Wong NL, Li Y, Au KW, Guo D, Xu J, Siu CW, Pei D, Tse HF, Esteban MA. Generation of induced pluripotent stem cell lines from 3 distinct laminopathies bearing heterogeneous mutations in lamin A/C. *Aging*. 2011;3:380–390.
18. Siu CW, Lee YK, Ho JC, Lai WH, Chan YC, Ng KM, Wong LY, Au KW, Lau YM, Zhang J, Lay KW, Colman A, Tse HF. Modeling of lamin A/C mutation premature cardiac aging using patient-specific induced pluripotent stem cells. *Aging*. 2012;4:803–822.
19. Lee YK, Ho PW, Schick R, Lau YM, Lai WH, Zhou T, Li Y, Ng KM, Ho SL, Esteban MA, Binah O, Tse HF, Siu CW. Modeling of Friedreich ataxia–related iron overloading cardiomyopathy using patient-specific-induced pluripotent stem cells. *Pflugers Arch*. 2014;466:1831–1844.
20. Sayed N, Liu C, Wu JC. Translation of human-induced pluripotent stem cells: from clinical trial in a dish to precision medicine. *J Am Coll Cardiol*. 2016;67:2161–2176.
21. Lai WH, Ho JC, Lee YK, Ng KM, Au KW, Chan YC, Lau CP, Tse HF, Siu CW. Rock inhibition facilitates the generation of human-induced pluripotent stem cells in a defined, feeder-, and serum-free system. *Cell Reprogram*. 2010;12:641–653.
22. Lian X, Zhang J, Azarin SM, Zhu K, Hazeltine LB, Bao X, Hsiao C, Kamp TJ, Palecek SP. Directed cardiomyocyte differentiation from human pluripotent stem cells by modulating Wnt/β-catenin signaling under fully defined conditions. *Nat Protoc*. 2013;8:162–175.
23. Kuramochi Y, Guo X, Sawyer DB, Lim CC. Rapid electrical stimulation induces early activation of kinase signal transduction pathways and apoptosis in adult rat ventricular myocytes. *Exp Physiol*. 2006;91:773–780.
24. Ho JC, Lai WH, Li MF, Au KW, Yip MC, Wong NL, Ng ES, Lam FF, Siu CW, Tse HF. Reversal of endothelial progenitor cell dysfunction in patients with type 2 diabetes using a conditioned medium of human embryonic stem cell-derived endothelial cells. *Diabetes Metab Res Rev*. 2012;28:462–473.
25. Chan YC, Ting S, Lee YK, Ng KM, Zhang J, Chen Z, Siu CW, Oh SK, Tse HF. Electrical stimulation promotes maturation of cardiomyocytes derived from human embryonic stem cells. *J Cardiovasc Transl Res*. 2013;6:989–999.
26. Ng KM, Lee YK, Lai WH, Chan YC, Fung ML, Tse HF, Siu CW. Exogenous expression of human apoA-I enhances cardiac differentiation of pluripotent stem cells. *PLoS One*. 2011;6:e19787.
27. Saga A, Karibe A, Otomo J, Iwabuchi K, Takahashi T, Kanno H, Kikuchi J, Keitoku M, Shinozaki T, Shimokawa H. Lamin A/C gene mutations in familial cardiomyopathy with advanced atrioventricular block and arrhythmia. *Tohoku J Exp Med*. 2009;218:309–316.
28. van Tintelen JP, Hofstra RM, Katerberg H, Rossenbacker T, Wiesfeld AC, du Marchie Sarvaas GJ, Wilde AA, van Langen IM, Nannenberg EA, van der Kooi AJ, Kraak M, van Gelder IC, van Veldhuisen DJ, Vos Y, van den Berg MP; Working Group on Inherited Cardiac Disorders, line 27/50, Interuniversity Cardiology Institute of The Netherlands . High yield of LMNA mutations in patients with dilated cardiomyopathy and/or conduction disease referred to cardiogenetics outpatient clinics. *Am Heart J*. 2007;154:1130–1139.
29. Nikolova V, Leimena C, McMahon AC, Tan JC, Chandar S, Jogia D, Kesteven SH, Michalicek J, Otway R, Verheyen F, Rainer S, Stewart CL, Martin D, Feneley MP, Fatkin D. Defects in nuclear structure and function promote dilated cardiomyopathy in lamin A/C-deficient mice. *J Clin Invest*. 2004;113:357–369.
30. Righolt CH, van't Hoff ML, Vermolen BJ, Young IT, Raz V. Robust nuclear lamina-based cell classification of aging and senescent cells. *Aging*. 2011;3:1192–1201.
31. Mendell JT, Dietz HC. When the message goes awry: disease-producing mutations that influence mRNA content and performance. *Cell*. 2001;107:411–414.
32. National Institutes of Health. Precision medicine initiative cohort program. https://www-nih-gov.eproxy1.lib.hku.hk/precision-medicine-initiative-cohort-program. Accessed January 13, 2016.
33. Collins FS, Varmus H. A new initiative on precision medicine. *N Engl J Med*. 2015;372:793–795.
34. Kosmidis G, Veerman CC, Casini S, Verkerk AO, van de Pas S, Bellin M, Wilde AA, Mummery CL, Bezzina CR. Readthrough-promoting drugs gentamicin and PTC124 fail to rescue Nav1.5 function of human-induced pluripotent stem cell-derived cardiomyocytes carrying nonsense mutations in the sodium channel gene *SCN5A*. *Circ Arrhythm Electrophysiol*. 2016;9:e004227.

SUPPLEMENTAL MATERIAL

Table S1. Raw data of apoptotic assay of the effects of PTC124 on electrically-stressed hiPSC-CMs by Apo-BrdU-TUNEL FACS analysis

Cell line	Treatment group	Number of cell		% of Apoptotic cell
		Total	Apoptotic (TUNEL-positive)	
$LMNA^{WT/WT}$	Control	1655	136	8.20
		1604	113	7.00
		1181	134	11.30
		650	72	11.10
		1505	211	14.00
		1546	140	9.10
		2457	129	5.30
	Electrically stressed	693	129	18.80
		8679	132	1.50
		1265	60	4.70
	Electrically stressed + PTC124	776	10	14.20
		1360	10	0.70
		8640	210	2.40
$LMNA^{R225X/WT}$	Control	1587	132	8.30
		4923	1653	38.50
		260	132	50.80
		2736	291	10.60
		3973	343	8.60
		692	131	18.90
		1532	826	53.90
	Electrically stressed	3642	1547	42.50
		272	196	72.10
		2062	1822	88.40
	Electrically stressed + PTC124	272	196	37.10
		2293	415	18.10
		8282	1572	19.00
		875	168	19.20
		152	54	35.50
$LMNA^{Q354X/WT}$	Control	689	75	10.90
		953	108	11.30
		395	54	13.70
		278	198	71.20
		2003	565	28.90
		1909	311	16.30
		593	75	12.60
		1385	533	38.50
	Electrically stressed	149	110	73.80
		2780	625	22.50
		1052	350	33.30
	Electrically stressed + PTC124	900	314	34.90
		1615	453	28.00
		2500	750	30.00
$LMNA^{T518fs/WT}$	Control	128	97	75.80
		220	124	56.40
		2266	1708	75.40
		1474	332	22.50
		1200	286	23.80
	Electrically stressed	608	321	52.80
		3549	543	15.30
		1426	342	24.00
	Electrically stressed + PTC124	261	207	79.30
		2255	413	18.30
		1152	415	36.00

Figure S1.

A Translation of *LMNA* wild type transcript (NM_170707)

```
1     atg gag acc ccg tcc cag cgg cgc gcc acc cgc agc ggg gcg cag   45
1     Met Glu Thr Pro Ser Gln Arg Arg Ala Thr Arg Ser Gly Ala Gln   15

46    gcc agc tcc act ccg ctg tcg ccc acc cgc atc acc cgg ctg cag   90
16    Ala Ser Ser Thr Pro Leu Ser Pro Thr Arg Ile Thr Arg Leu Gln   30

91    gag aag gag gac ctg cag gag ctc aat gat cgc ttg gcg gtc tac   135
31    Glu Lys Glu Asp Leu Gln Glu Leu Asn Asp Arg Leu Ala Val Tyr   45

136   atc gac cgt gtg cgc tcg ctg gaa acg gag aac gca ggg ctg cgc   180
46    Ile Asp Arg Val Arg Ser Leu Glu Thr Glu Asn Ala Gly Leu Arg   60

181   ctt cgc atc acc gag tct gaa gag gtg gtc agc cgc gag gtg tcc   225
61    Leu Arg Ile Thr Glu Ser Glu Glu Val Val Ser Arg Glu Val Ser   75

226   ggc atc aag gcc gcc tac gag gcc gag ctc ggg gat gcc cgc aag   270
76    Gly Ile Lys Ala Ala Tyr Glu Ala Glu Leu Gly Asp Ala Arg Lys   90

271   acc ctt gac tca gta gcc aag gag cgc gcc cgc ctg cag ctg gag   315
91    Thr Leu Asp Ser Val Ala Lys Glu Arg Ala Arg Leu Gln Leu Glu   105

316   ctg agc aaa gtg cgt gag gag ttt aag gag ctg aaa gcg cgc aat   360
106   Leu Ser Lys Val Arg Glu Glu Phe Lys Glu Leu Lys Ala Arg Asn   120

361   acc aag aag gag ggt gac ctg ata gct gct cag gct cgg ctg aag   405
121   Thr Lys Lys Glu Gly Asp Leu Ile Ala Ala Gln Ala Arg Leu Lys   135

406   gac ctg gag gct ctg ctg aac tcc aag gag gcc gca ctg agc act   450
136   Asp Leu Glu Ala Leu Leu Asn Ser Lys Glu Ala Ala Leu Ser Thr   150

451   gct ctc agt gag aag cgc acg ctg gag ggc gag ctg cat gat ctg   495
151   Ala Leu Ser Glu Lys Arg Thr Leu Glu Gly Glu Leu His Asp Leu   165

496   cgg ggc cag gtg gcc aag ctt gag gca gcc cta ggt gag gcc aag   540
166   Arg Gly Gln Val Ala Lys Leu Glu Ala Ala Leu Gly Glu Ala Lys   180

541   aag caa ctt cag gat gag atg ctg cgg cgg gtg gat gct gag aac   585
181   Lys Gln Leu Gln Asp Glu Met Leu Arg Arg Val Asp Ala Glu Asn   195

586   agg ctg cag acc atg aag gag gaa ctg gac ttc cag aag aac atc   630
196   Arg Leu Gln Thr Met Lys Glu Glu Leu Asp Phe Gln Lys Asn Ile   210

631   tac agt gag gag ctg cgt gag acc aag cgc cgt cat gag acc cga   675
211   Tyr Ser Glu Glu Leu Arg Glu Thr Lys Arg Arg His Glu Thr Arg   225

676   ctg gtg gag att gac aat ggg aag cag cgt gag ttt gag agc cgg   720
226   Leu Val Glu Ile Asp Asn Gly Lys Gln Arg Glu Phe Glu Ser Arg   240

721   ctg gcg gat gcg ctg cag gaa ctg cgg gcc cag cat gag gac cag   765
241   Leu Ala Asp Ala Leu Gln Glu Leu Arg Ala Gln His Glu Asp Gln   255

766   gtg gag cag tat aag aag gag ctg gag aag act tat tct gcc aag   810
256   Val Glu Gln Tyr Lys Lys Glu Leu Glu Lys Thr Tyr Ser Ala Lys   270

811   ctg gac aat gcc agg cag tct gct gag agg aac agc aac ctg gtg   855
271   Leu Asp Asn Ala Arg Gln Ser Ala Glu Arg Asn Ser Asn Leu Val   285

856   ggg gct gcc cac gag gag ctg cag cag tcg cgc atc cgc atc gac   900
286   Gly Ala Ala His Glu Glu Leu Gln Gln Ser Arg Ile Arg Ile Asp   300

901   agc ctc tct gcc cag ctc agc cag ctc cag aag cag ctg gca gcc   945
301   Ser Leu Ser Ala Gln Leu Ser Gln Leu Gln Lys Gln Leu Ala Ala   315

946   aag gag gcg aag ctt cga gac ctg gag gac tca ctg gcc cgt gag   990
316   Lys Glu Ala Lys Leu Arg Asp Leu Glu Asp Ser Leu Ala Arg Glu   330

991   cgg gac acc agc cgg cgg ctg ctg gcg gaa aag gag cgg gag atg   1035
331   Arg Asp Thr Ser Arg Arg Leu Leu Ala Glu Lys Glu Arg Glu Met   345

1036  gcc gag atg cgg gca agg atg cag cag cag ctg gac gag tac cag   1080
346   Ala Glu Met Arg Ala Arg Met Gln Gln Gln Leu Asp Glu Tyr Gln   360

1081  gag ctt ctg gac atc aag ctg gcc ctg gac atg gag atc cac gcc   1125
361   Glu Leu Leu Asp Ile Lys Leu Ala Leu Asp Met Glu Ile His Ala   375

1126  tac cgc aag ctc ttg gag ggc gag gag gag agg cta cgc ctg tcc   1170
376   Tyr Arg Lys Leu Leu Glu Gly Glu Glu Glu Arg Leu Arg Leu Ser   390

1171  ccc agc cct acc tcg cag cgc agc cgt ggc cgt gct tcc tct cac   1215
391   Pro Ser Pro Thr Ser Gln Arg Ser Arg Gly Arg Ala Ser Ser His   405

1216  tca tcc cag aca cag ggt ggg ggc agc gtc acc aaa aag cgc aaa   1260
406   Ser Ser Gln Thr Gln Gly Gly Gly Ser Val Thr Lys Lys Arg Lys   420

1261  ctg gag tcc act gag agc cgc agc agc ttc tca cag cac gca cgc   1305
421   Leu Glu Ser Thr Glu Ser Arg Ser Ser Phe Ser Gln His Ala Arg   435

1306  act agc ggg cgc gtg gcc gtg gag gag gtg gat gag gag ggc aag   1350
436   Thr Ser Gly Arg Val Ala Val Glu Glu Val Asp Glu Glu Gly Lys   450

1351  ttt gtc cgg ctg cgc aac aag tcc aat gag gac cag tcc atg ggc   1395
451   Phe Val Arg Leu Arg Asn Lys Ser Asn Glu Asp Gln Ser Met Gly   465

1396  aat tgg cag atc aag cgc cag aat gga gat gat ccc ttg ctg act   1440
466   Asn Trp Gln Ile Lys Arg Gln Asn Gly Asp Asp Pro Leu Leu Thr   480

1441  tac cgg ttc cca cca aag ttc acc ctg aag gct ggg cag gtg gtg   1485
481   Tyr Arg Phe Pro Pro Lys Phe Thr Leu Lys Ala Gly Gln Val Val   495

1486  acg atc tgg gct gca gga gct ggg gcc acc cac agc ccc cct acc   1530
496   Thr Ile Trp Ala Ala Gly Ala Gly Ala Thr His Ser Pro Pro Thr   510
                                      T518
1531  gac ctg gtg tgg aag gca cag aac acc tgg ggc tgc ggg aac agc   1575
511   Asp Leu Val Trp Lys Ala Gln Asn Thr Trp Gly Cys Gly Asn Ser   525

1576  ctg cgt acg gct ctc atc aac tcc act ggg gaa gaa gtg gcc atg   1620
526   Leu Arg Thr Ala Leu Ile Asn Ser Thr Gly Glu Glu Val Ala Met   540

1621  cgc aag ctg gtg cgc tca gtg act gtg gtt gag gac gac gag gat   1665
541   Arg Lys Leu Val Arg Ser Val Thr Val Val Glu Asp Asp Glu Asp   555

1666  gag gat gga gat gac ctg ctc cat cac cac cac ggc tcc cac tgc   1710
556   Glu Asp Gly Asp Asp Leu Leu His His His His Gly Ser His Cys   570

1711  agc agc tcg ggg gac ccc gct gag tac aac ctg cgc tcg cgc acc   1755
571   Ser Ser Ser Gly Asp Pro Ala Glu Tyr Asn Leu Arg Ser Arg Thr   585

1756  gtg ctg tgc ggg acc tgc ggg cag cct gcc gac aag gca tct gcc   1800
586   Val Leu Cys Gly Thr Cys Gly Gln Pro Ala Asp Lys Ala Ser Ala   600

1801  agc ggc tca gga gcc cag gtg ggc gga ccc atc tcc tct ggc tct   1845
601   Ser Gly Ser Gly Ala Gln Val Gly Gly Pro Ile Ser Ser Gly Ser   615

1846  tct gcc tcc agt gtc acg gtc act cgc agc tac cgc agt gtg ggg   1890
616   Ser Ala Ser Ser Val Thr Val Thr Arg Ser Tyr Arg Ser Val Gly   630

1891  ggc agt ggg ggt ggc agc ttc ggg gac aat ctg gtc acc cgc tcc   1935
631   Gly Ser Gly Gly Gly Ser Phe Gly Asp Asn Leu Val Thr Arg Ser   645

1936  tac ctc ctg ggc aac tcc agc ccc cga acc cag agc ccc cag aac   1980
646   Tyr Leu Leu Gly Asn Ser Ser Pro Arg Thr Gln Ser Pro Gln Asn   660

1981  tgc agc atc atg taa   1995
661   Cys Ser Ile Met End   665
```

Yellow: Start codon
Blue: Frameshift mutation site due to deletion
Red: Stop codon

B Translation of *LMNA* T518 frameshit mutation transcript

```
1     atg gag acc ccg tcc cag cgg cgc gcc acc cgc agc ggg gcg cag   45
1     Met Glu Thr Pro Ser Gln Arg Arg Ala Thr Arg Ser Gly Ala Gln   15

46    gcc agc tcc act ccg ctg tcg ccc acc cgc atc acc cgg ctg cag   90
16    Ala Ser Ser Thr Pro Leu Ser Pro Thr Arg Ile Thr Arg Leu Gln   30

91    gag aag gag gac ctg cag gag ctc aat gat cgc ttg gcg gtc tac   135
31    Glu Lys Glu Asp Leu Gln Glu Leu Asn Asp Arg Leu Ala Val Tyr   45

136   atc gac cgt gtg cgc tcg ctg gaa acg gag aac gca ggg ctg cgc   180
46    Ile Asp Arg Val Arg Ser Leu Glu Thr Glu Asn Ala Gly Leu Arg   60

181   ctt cgc atc acc gag tct gaa gag gtg gtc agc cgc gag gtg tcc   225
61    Leu Arg Ile Thr Glu Ser Glu Glu Val Val Ser Arg Glu Val Ser   75

226   ggc atc aag gcc gcc tac gag gcc gag ctc ggg gat gcc cgc aag   270
76    Gly Ile Lys Ala Ala Tyr Glu Ala Glu Leu Gly Asp Ala Arg Lys   90

271   acc ctt gac tca gta gcc aag gag cgc gcc cgc ctg cag ctg gag   315
91    Thr Leu Asp Ser Val Ala Lys Glu Arg Ala Arg Leu Gln Leu Glu   105

316   ctg agc aaa gtg cgt gag gag ttt aag gag ctg aaa gcg cgc aat   360
106   Leu Ser Lys Val Arg Glu Glu Phe Lys Glu Leu Lys Ala Arg Asn   120

361   acc aag aag gag ggt gac ctg ata gct gct cag gct cgg ctg aag   405
121   Thr Lys Lys Glu Gly Asp Leu Ile Ala Ala Gln Ala Arg Leu Lys   135

406   gac ctg gag gct ctg ctg aac tcc aag gag gcc gca ctg agc act   450
136   Asp Leu Glu Ala Leu Leu Asn Ser Lys Glu Ala Ala Leu Ser Thr   150

451   gct ctc agt gag aag cgc acg ctg gag ggc gag ctg cat gat ctg   495
151   Ala Leu Ser Glu Lys Arg Thr Leu Glu Gly Glu Leu His Asp Leu   165

496   cgg ggc cag gtg gcc aag ctt gag gca gcc cta ggt gag gcc aag   540
166   Arg Gly Gln Val Ala Lys Leu Glu Ala Ala Leu Gly Glu Ala Lys   180

541   aag caa ctt cag gat gag atg ctg cgg cgg gtg gat gct gag aac   585
181   Lys Gln Leu Gln Asp Glu Met Leu Arg Arg Val Asp Ala Glu Asn   195

586   agg ctg cag acc atg aag gag gaa ctg gac ttc cag aag aac atc   630
196   Arg Leu Gln Thr Met Lys Glu Glu Leu Asp Phe Gln Lys Asn Ile   210

631   tac agt gag gag ctg cgt gag acc aag cgc cgt cat gag acc cga   675
211   Tyr Ser Glu Glu Leu Arg Glu Thr Lys Arg Arg His Glu Thr Arg   225

676   ctg gtg gag att gac aat ggg aag cag cgt gag ttt gag agc cgg   720
226   Leu Val Glu Ile Asp Asn Gly Lys Gln Arg Glu Phe Glu Ser Arg   240

721   ctg gcg gat gcg ctg cag gaa ctg cgg gcc cag cat gag gac cag   765
241   Leu Ala Asp Ala Leu Gln Glu Leu Arg Ala Gln His Glu Asp Gln   255

766   gtg gag cag tat aag aag gag ctg gag aag act tat tct gcc aag   810
256   Val Glu Gln Tyr Lys Lys Glu Leu Glu Lys Thr Tyr Ser Ala Lys   270

811   ctg gac aat gcc agg cag tct gct gag agg aac agc aac ctg gtg   855
271   Leu Asp Asn Ala Arg Gln Ser Ala Glu Arg Asn Ser Asn Leu Val   285

856   ggg gct gcc cac gag gag ctg cag cag tcg cgc atc cgc atc gac   900
286   Gly Ala Ala His Glu Glu Leu Gln Gln Ser Arg Ile Arg Ile Asp   300

901   agc ctc tct gcc cag ctc agc cag ctc cag aag cag ctg gca gcc   945
301   Ser Leu Ser Ala Gln Leu Ser Gln Leu Gln Lys Gln Leu Ala Ala   315

946   aag gag gcg aag ctt cga gac ctg gag gac tca ctg gcc cgt gag   990
316   Lys Glu Ala Lys Leu Arg Asp Leu Glu Asp Ser Leu Ala Arg Glu   330

991   cgg gac acc agc cgg cgg ctg ctg gcg gaa aag gag cgg gag atg   1035
331   Arg Asp Thr Ser Arg Arg Leu Leu Ala Glu Lys Glu Arg Glu Met   345

1036  gcc gag atg cgg gca agg atg cag cag cag ctg gac gag tac cag   1080
346   Ala Glu Met Arg Ala Arg Met Gln Gln Gln Leu Asp Glu Tyr Gln   360

1081  gag ctt ctg gac atc aag ctg gcc ctg gac atg gag atc cac gcc   1125
361   Glu Leu Leu Asp Ile Lys Leu Ala Leu Asp Met Glu Ile His Ala   375

1126  tac cgc aag ctc ttg gag ggc gag gag gag agg cta cgc ctg tcc   1170
376   Tyr Arg Lys Leu Leu Glu Gly Glu Glu Glu Arg Leu Arg Leu Ser   390

1171  ccc agc cct acc tcg cag cgc agc cgt ggc cgt gct tcc tct cac   1215
391   Pro Ser Pro Thr Ser Gln Arg Ser Arg Gly Arg Ala Ser Ser His   405

1216  tca tcc cag aca cag ggt ggg ggc agc gtc acc aaa aag cgc aaa   1260
406   Ser Ser Gln Thr Gln Gly Gly Gly Ser Val Thr Lys Lys Arg Lys   420

1261  ctg gag tcc act gag agc cgc agc agc ttc tca cag cac gca cgc   1305
421   Leu Glu Ser Thr Glu Ser Arg Ser Ser Phe Ser Gln His Ala Arg   435

1306  act agc ggg cgc gtg gcc gtg gag gag gtg gat gag gag ggc aag   1350
436   Thr Ser Gly Arg Val Ala Val Glu Glu Val Asp Glu Glu Gly Lys   450

1351  ttt gtc cgg ctg cgc aac aag tcc aat gag gac cag tcc atg ggc   1395
451   Phe Val Arg Leu Arg Asn Lys Ser Asn Glu Asp Gln Ser Met Gly   465

1396  aat tgg cag atc aag cgc cag aat gga gat gat ccc ttg ctg act   1440
466   Asn Trp Gln Ile Lys Arg Gln Asn Gly Asp Asp Pro Leu Leu Thr   480

1441  tac cgg ttc cca cca aag ttc acc ctg aag gct ggg cag gtg gtg   1485
481   Tyr Arg Phe Pro Pro Lys Phe Thr Leu Lys Ala Gly Gln Val Val   495

1486  acg atc tgg gct gca gga gct ggg gcc acc cac agc ccc cct acc   1530
496   Thr Ile Trp Ala Ala Gly Ala Gly Ala Thr His Ser Pro Pro Thr   510
                                  c.1554delC; p.T518fs
1531  gac ctg gtg tgg aag gca cag aac act ggg gct gcg gga aca gcc   1575
511   Asp Leu Val Trp Lys Ala Gln Asn Thr Gly Ala Ala Gly Thr Ala   525

1577  tgc gta cgg ctc tca tca act cca ctg ggg aag aag tgg cca tgc   1621
526   Cys Val Arg Leu Ser Ser Thr Pro Leu Gly Lys Lys Trp Pro Cys   540

1622  gca agc tgg tgc gct cag tga ctg tgg ttg aag acg acg aag atg   1666

541   Ala Ser Trp Cys Ala Gln End Leu Trp Leu Arg Thr Thr Arg Met   555
```

Premature stop codon

Yellow: Start codon
Blue: Frameshift mutation site due to deletion
Red: Stop codon

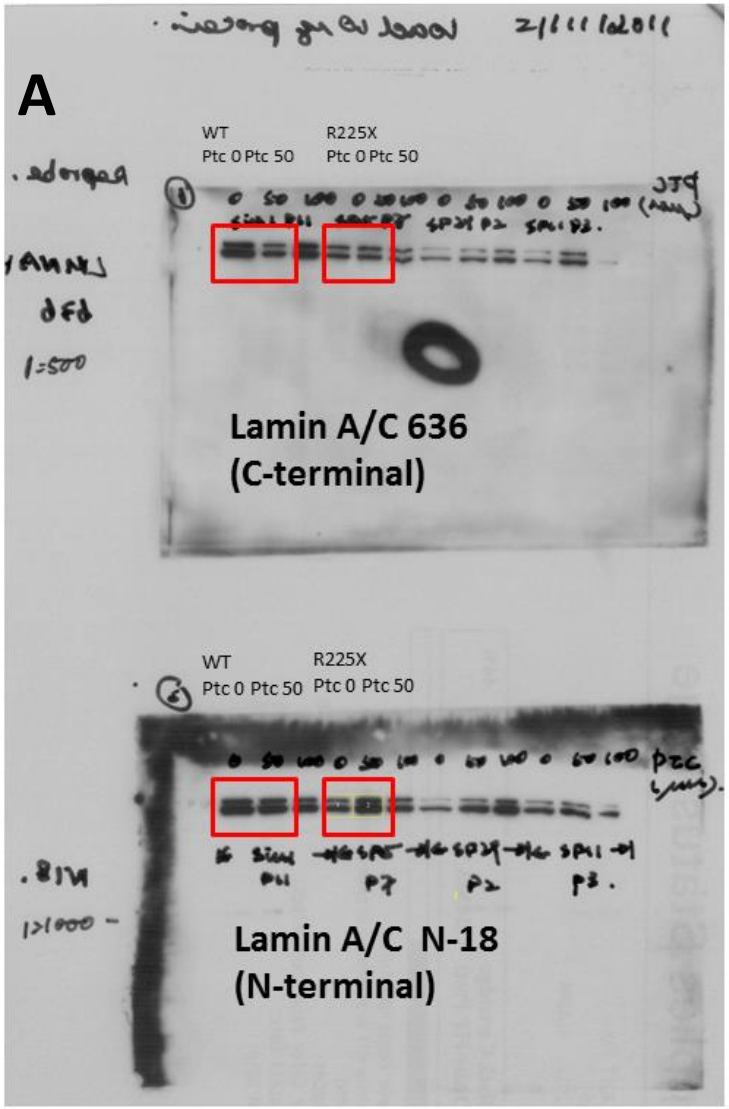

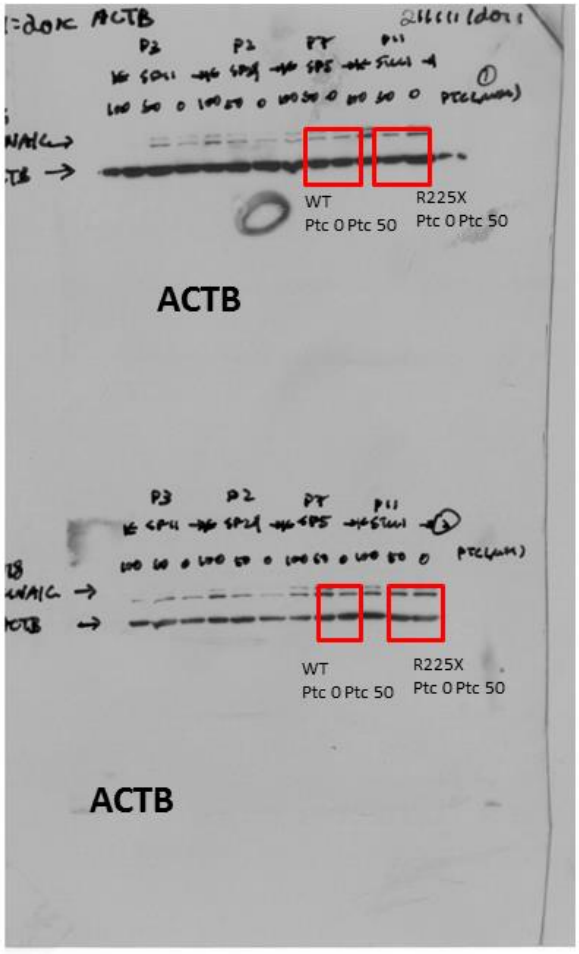

Skin fibroblast
21/11/2011

Figure S2. A.

B

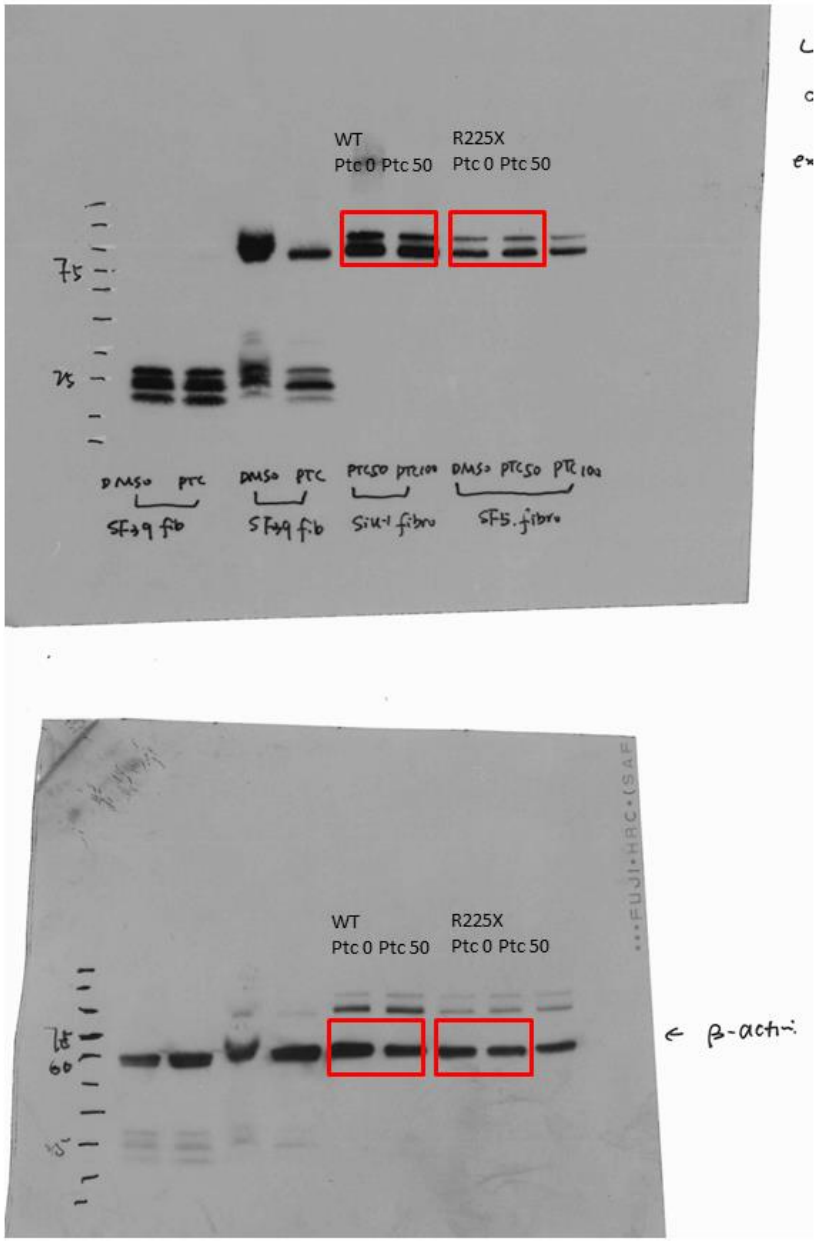

Skin fibroblast
6/12/2016
SF5: R225X;
Siu-1: WT

C

Skin fibroblast
SF5: R225X;
Siu-1: WT

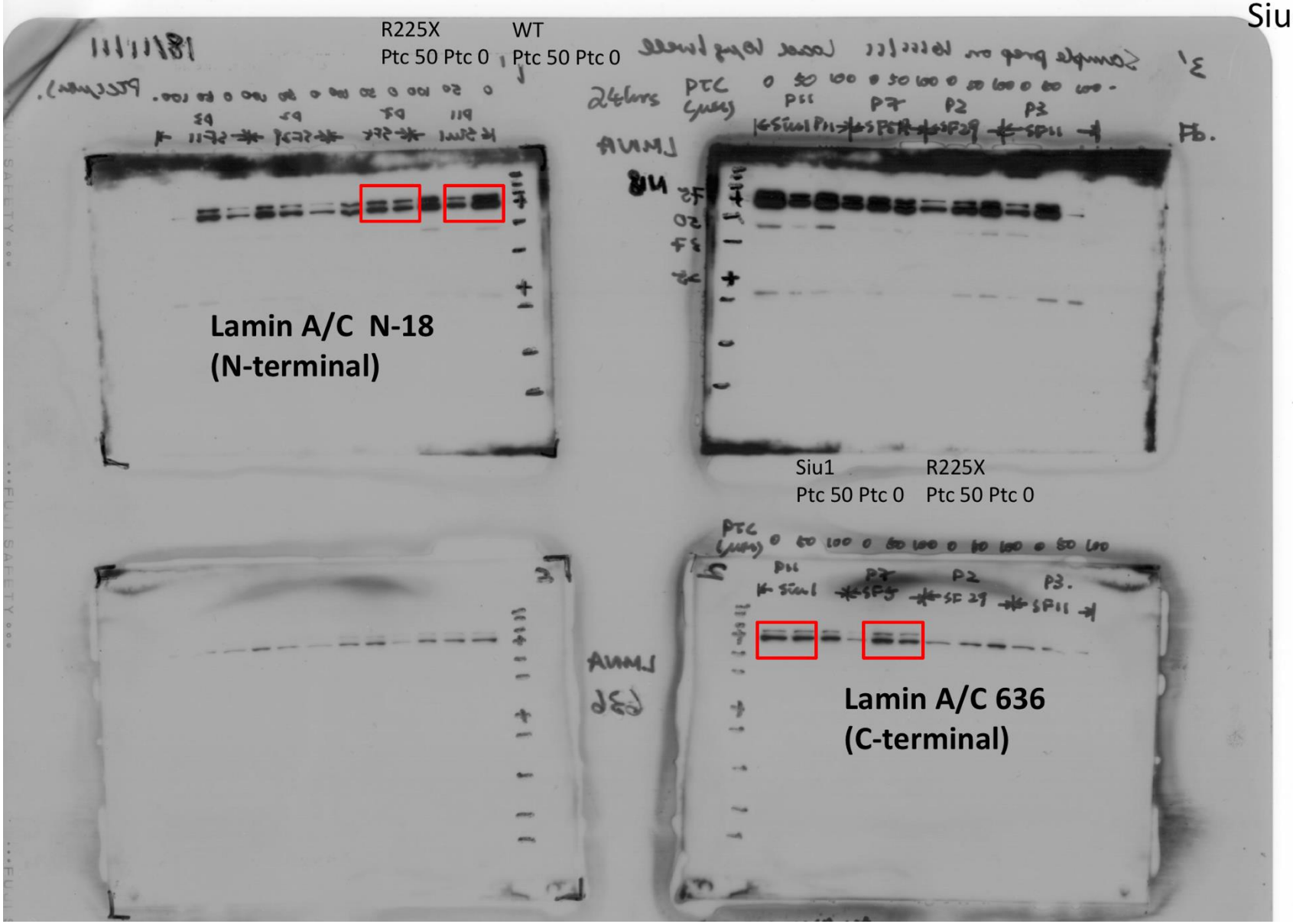

D

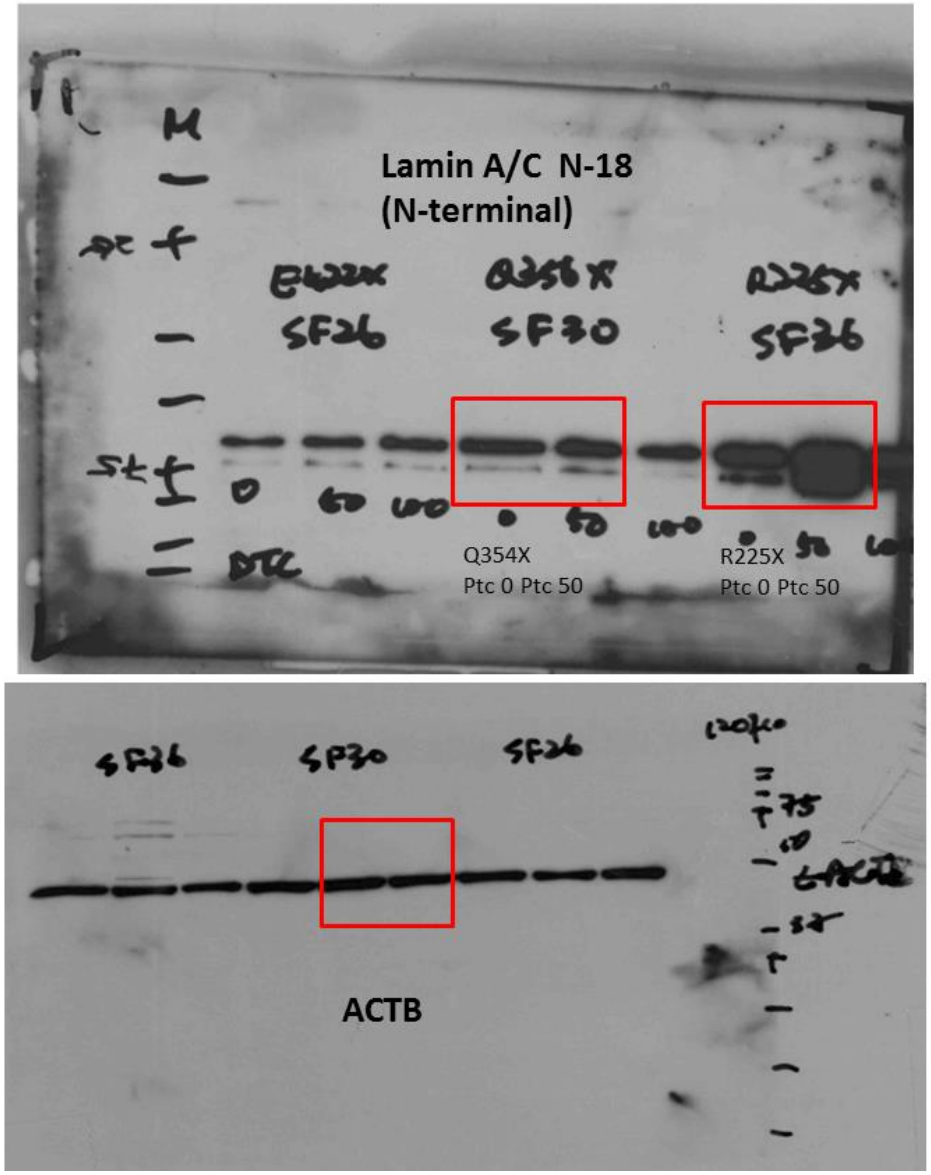

Skin fibroblast
19/6/12
Sf30 = Q354X

E

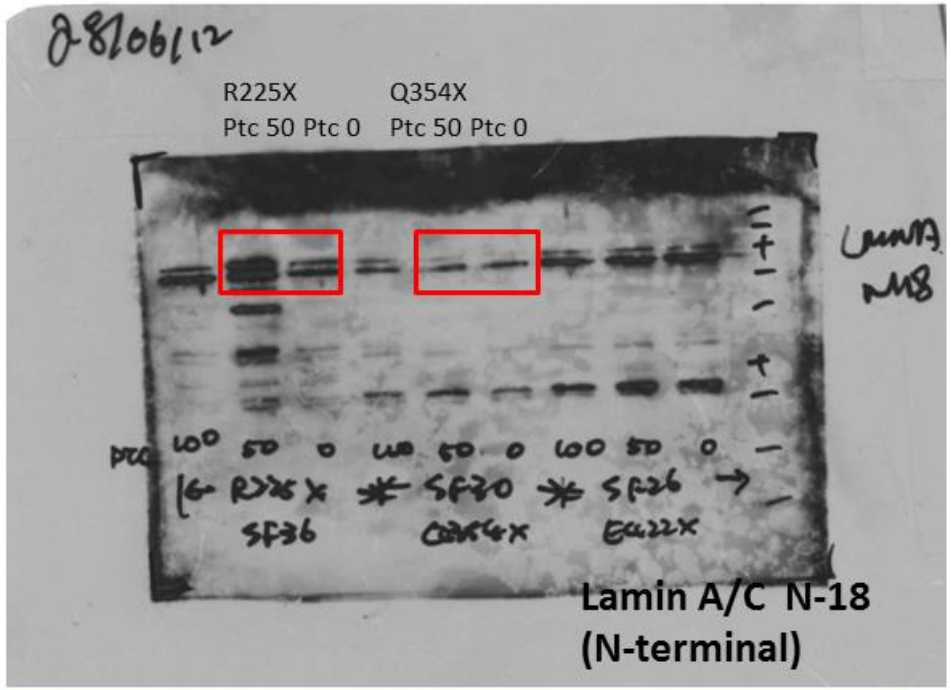

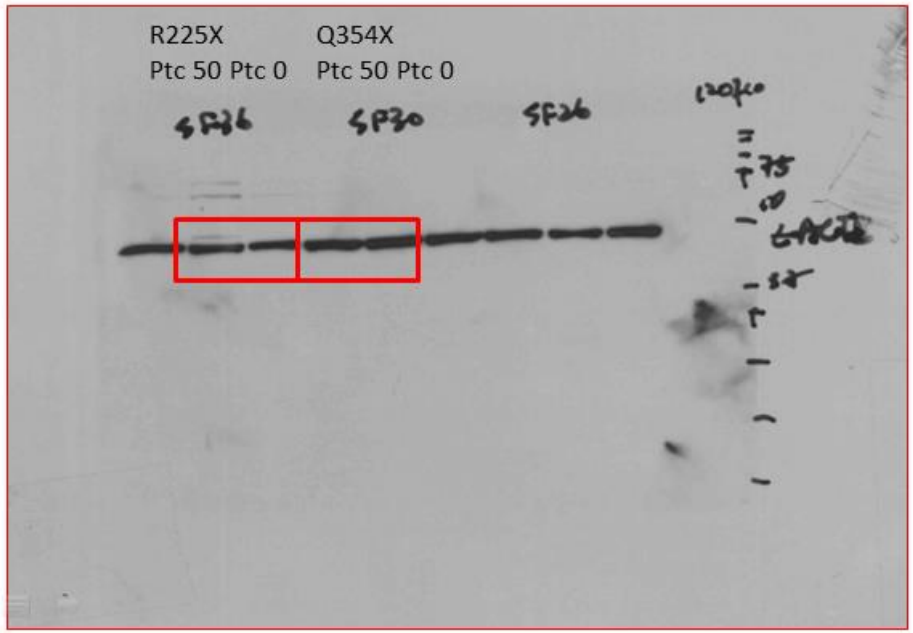

Skin fibroblast
SF36: R225X
SF30: Q354X

F

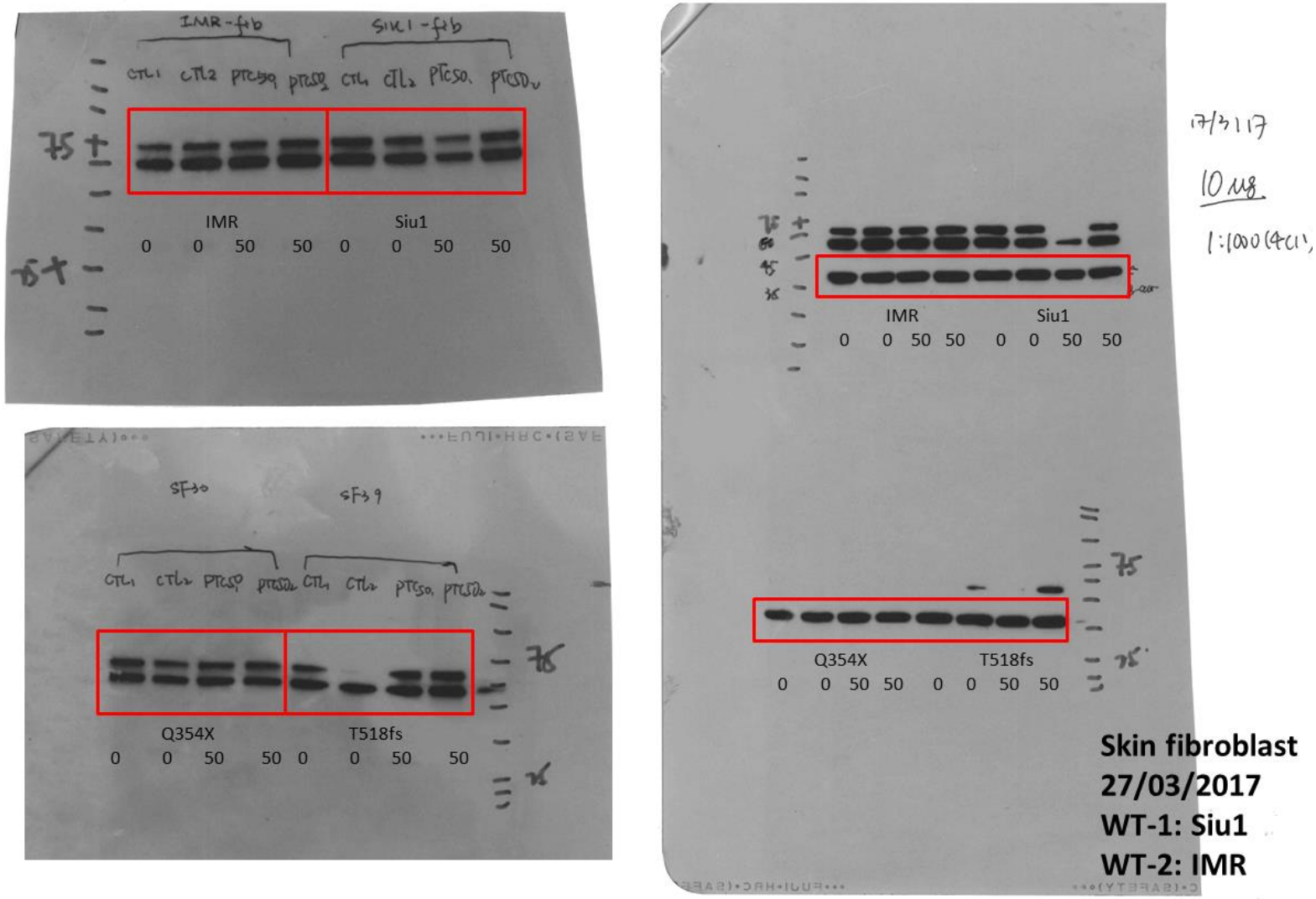
IMR-fib
Siu1-fib
CTL1 CTL2 PTCS9 PTCS9 CTL1 CTL2 PTCS0. PTCS0.
75
IMR
Siu1
0 0 50 50 0 0 50 50
SF30
SF39
CTL1 CTL2 PTCS0 PTCS0 CTL1 CTL2 PTCS0. PTCS0.
Q354X
T518fs
0 0 50 50 0 0 50 50
17/3/17
10 ug
1:1000(4C)
Skin fibroblast
27/03/2017
WT-1: Siu1
WT-2: IMR

G

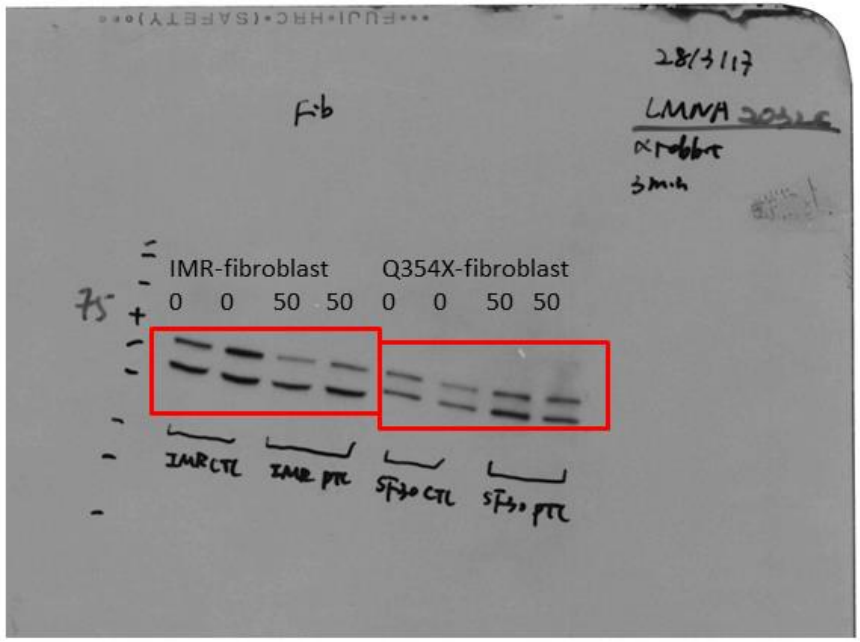

Lamin A/C N-18 (N-terminal)

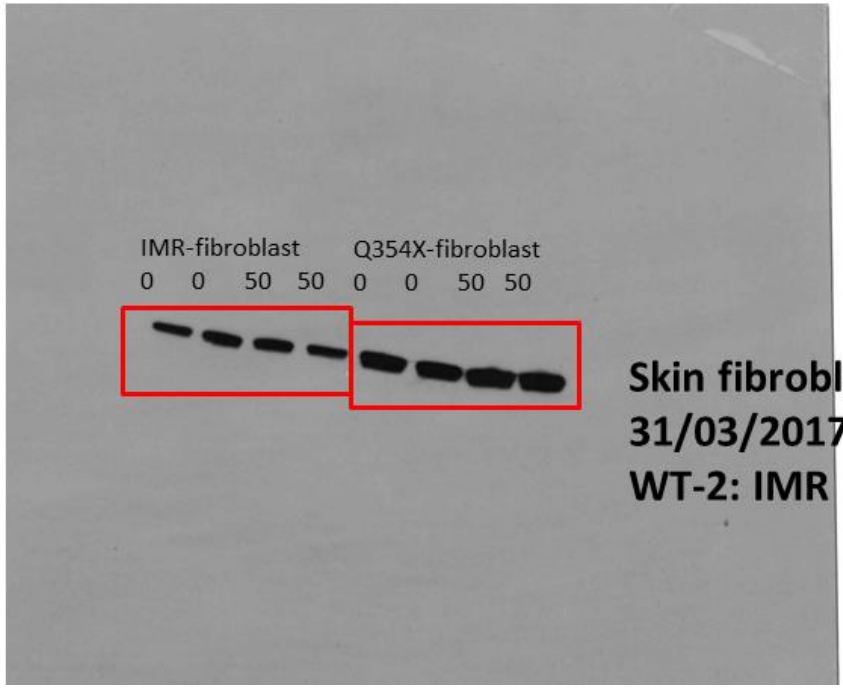

ACTB

Skin fibroblast
31/03/2017
WT-2: IMR

H

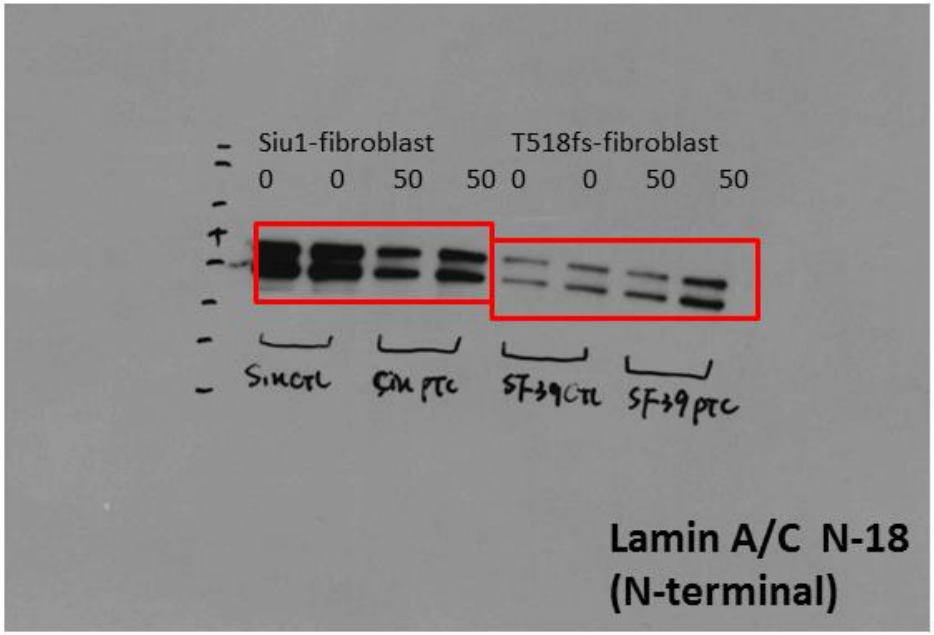

Skin fibroblast
27/03/2017
WT-2: IMR

I

19/8 hiPSC-CM

Sf 36 =Q354X
Sf 39 =T518fs

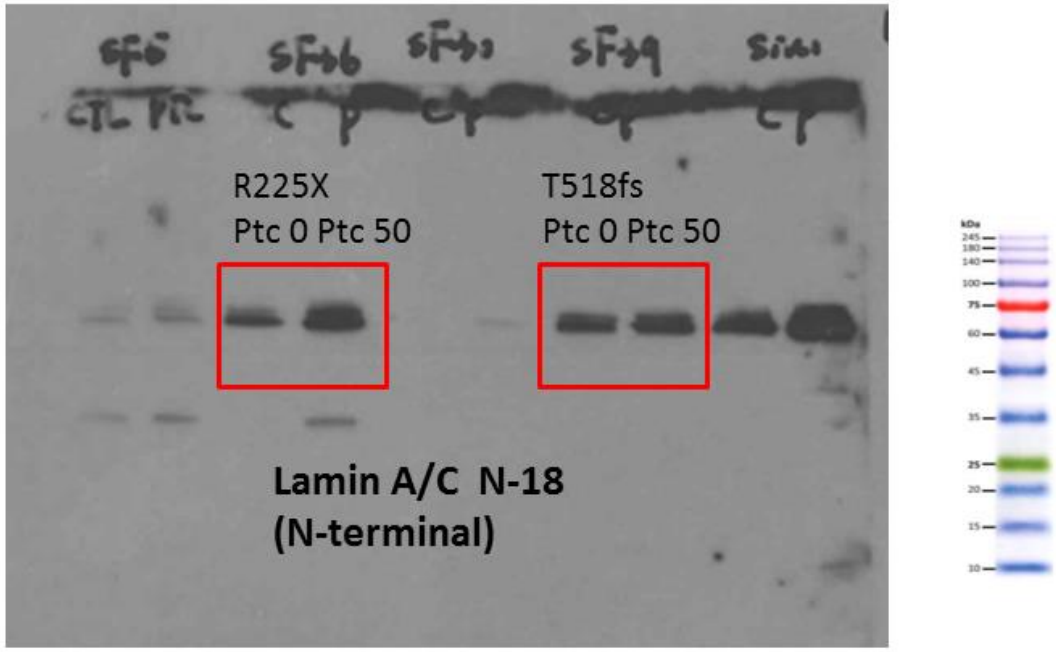

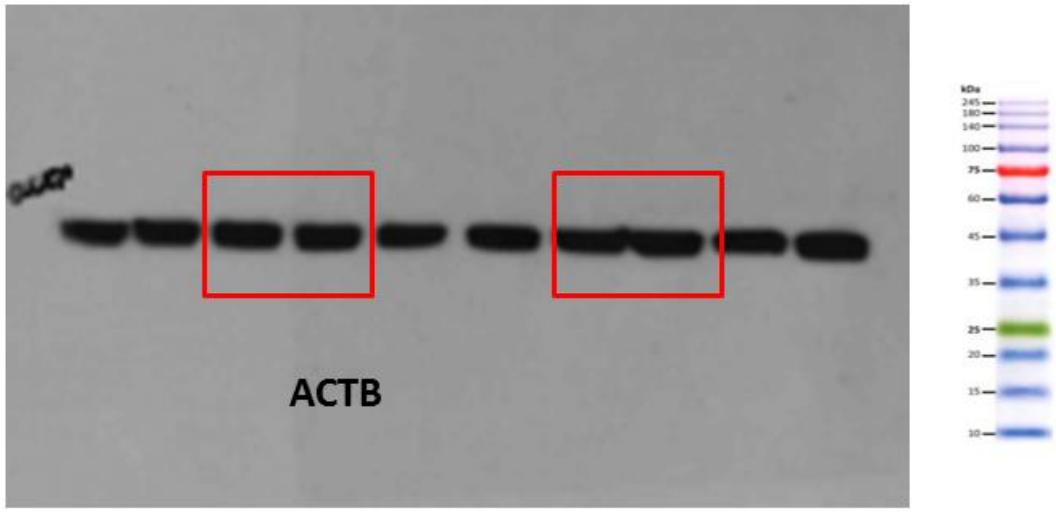

J

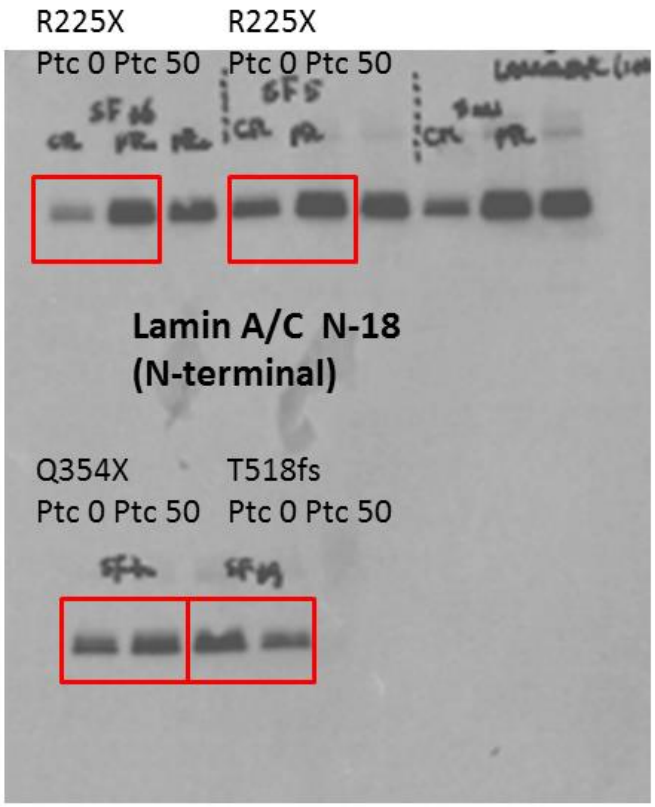

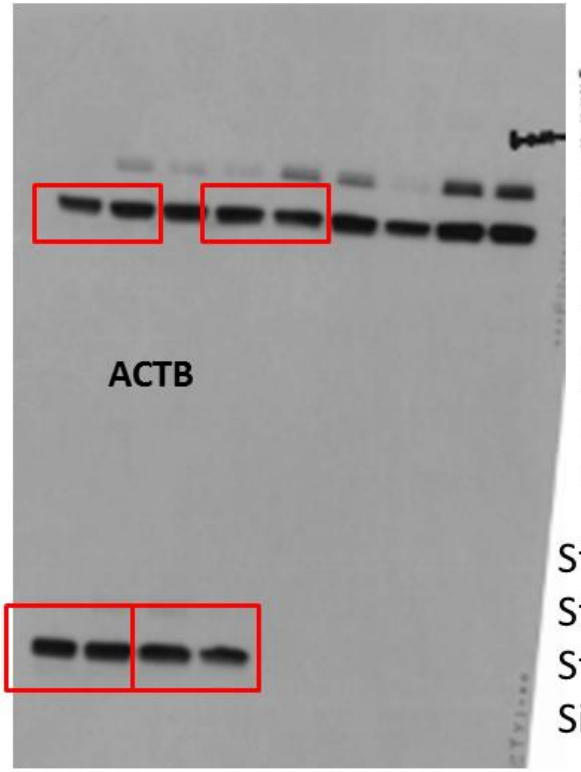

30/8 hiPSC-CM

Sf 5 & Sf 36: R225X
Sf 39: T518 fs
Sf30: Q354X
Siu: WT

K

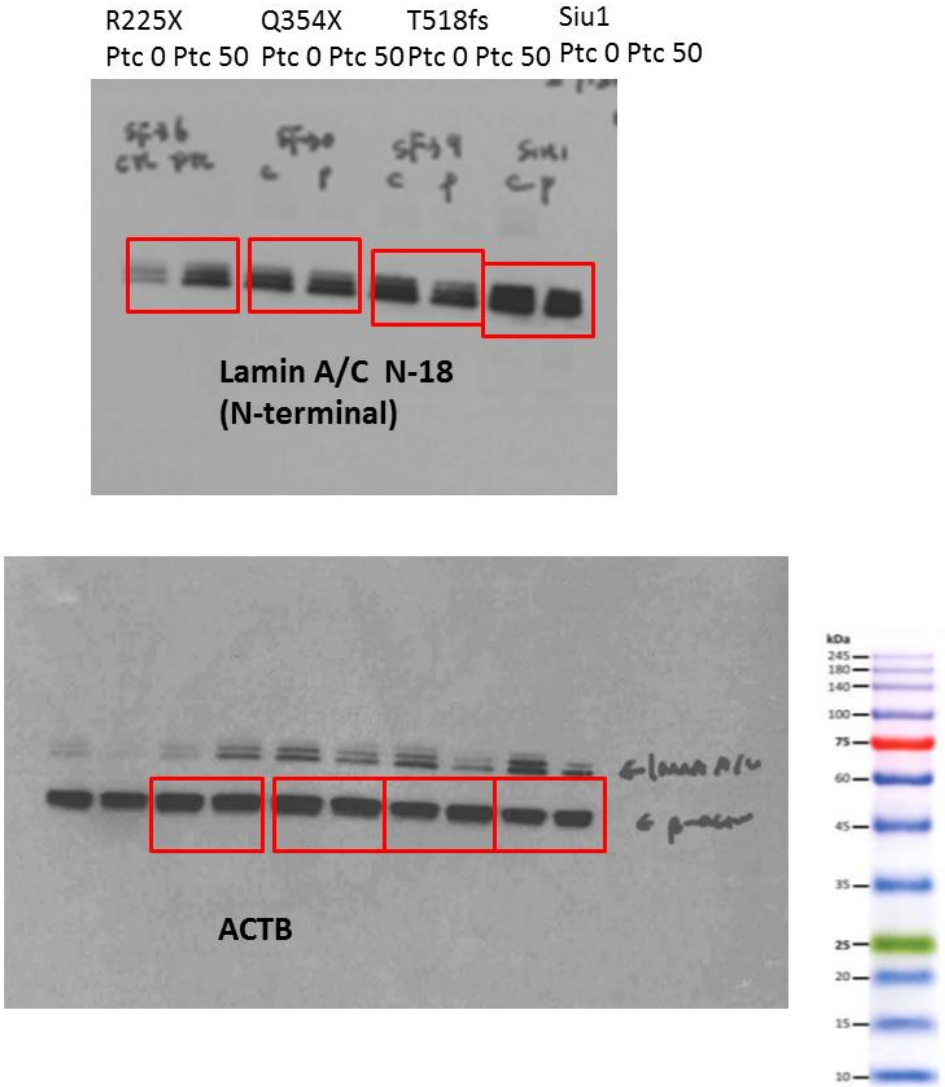

6/9 hiPSC-CM
Wt
Sf36 =R225X
Sf30 =Q354X
Sf39 =T518fs

L

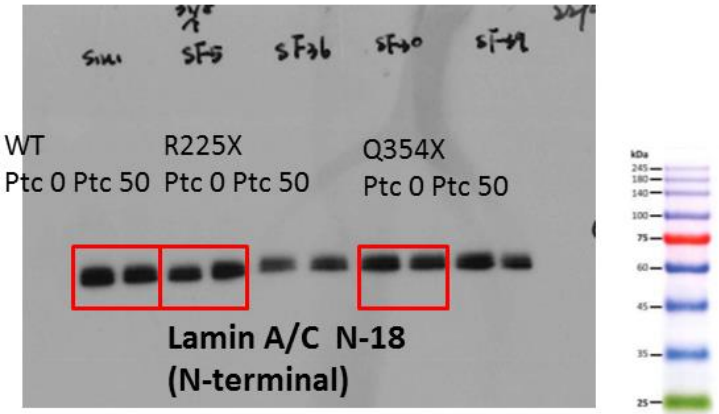

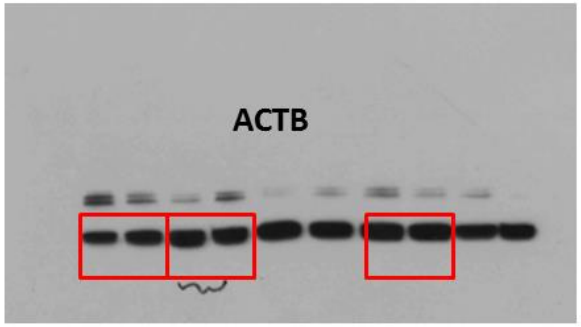

22/9 hiPSC-CM
Siu1: WT
Sf5-R225X
Sf30-Q354X

M

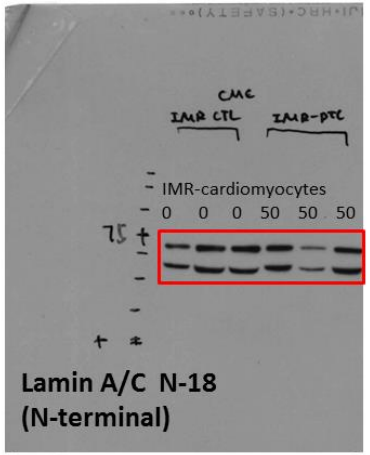

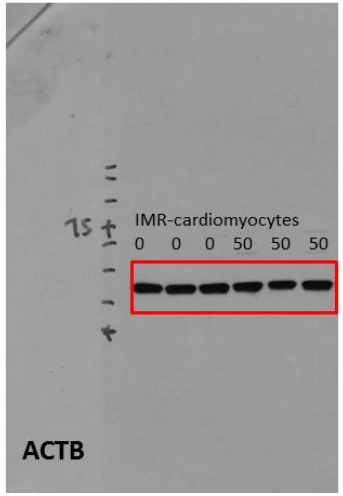

hiPSC-CM
31/03/2017
WT-2: IMR

Supplemental Figure Legends:

Figure S1. Translational product of *LMNA* T518fs mutated transcript. (A) Wild type *LMNA* mRNA transcript (NM_170707); (B) Prediction of second open reading frame (ORF) with one "c" deletion at the 1554th codon position in the *LMNA* mRNA transcript, the premature stop codon with sequence of "TGA" will be generated at an earlier position at the 547th amino acid, shortening of the Lmna protein that is supposed to be transcribed (reduced from the 665th to 547th amino acids). Moreover, even after PTC124 read-through, the amino acid sequence after frameshift mutation (the 519th amino acid) would be totally deviated from the native lamin A/C ones.

Figure S2. Effects of PTC124 on the expression of lamin A/C proteins in dermal fibroblasts (A-H) and hiPSC-derived cardiomyocytes (hiPSC-CMC) (I-M) derived from wild-type (*LMNA*$^{WT1/WT1}$ & *LMNA*$^{WT2/WT2}$) and *LMNA* mutants (*LMNA*$^{R225X/WT}$, *LMNA*$^{Q354X/WT}$ and *LMNA*$^{T518fs/WT}$). Original images of immunoblots with at least one wild type sample loaded on the same gel with patient samples. Lamin A/C (clone N18) were probed with antibody that recognized N-terminal, while beta-actin (ACTB) was used as the internal control for normalization of protein loading. Three to six independent samples were prepared for western blot analysis.